

addition, intravascular delivery was performed as a form of limb perfusion, in an attempt to bypass the immune activation of DCs in the injected muscle.<sup>12</sup> We investigated the transgene expression and host immune response to two distinct serotypes of rAAV in normal and dystrophic dogs after direct intramuscular injection and after limb perfusion.

## RESULTS

### Extensive expression of $\beta$ -galactosidase in rAAV8-transduced muscles in wild-type dogs

We administered nonincisional intramuscular injections under ultrasonographic guidance so as to minimize injury. With incisional injection, the ordinary method of intramuscular viral administration in dogs,<sup>8</sup> the skin is opened to identify the individual muscles. This may enhance the immune reaction by recruiting inflammatory cells for wound healing. After nonincisional injection of rAAV2-*lacZ*, faint  $\beta$ -galactosidase ( $\beta$ -gal) expression was detected, whereas lymphocyte infiltration still occurred (Supplementary Figure S1). To investigate the transduction efficiency of rAAV8 in canine skeletal muscle, normal dogs were transduced with rAAV-*lacZ* serotypes 2 and 8 (Table 1). Prominent expression of  $\beta$ -gal was observed in the rAAV8-*lacZ*-injected muscles, whereas the rAAV2-*lacZ*-injected muscles showed minimal transgene expression (Figure 1). While  $\beta$ -gal expression in the rAAV8-injected muscle was correlated with the viral dose,

$\beta$ -gal expression in the rAAV2-injected muscle was not augmented with viral dose escalation. However, rAAV8-*lacZ*-injected muscles, which showed extensive  $\beta$ -gal expression at 2 weeks, also exhibited reduced expression at 4 weeks after the injection, thereby suggesting that the transgene product had immunogenicity (Supplementary Figure S2).

To evaluate the difference in transduction efficiency between rAAV2 and rAAV8 at 2 weeks after the injection, relative quantifications of the vector genome and mRNA were performed. The result demonstrated higher transduction rates in the rAAV8-injected muscles as increasing amounts of the vector were administered (Figure 2a,b). The amount of protein expression was also well correlated with that of transgenic DNA (Figure 2c, Supplementary Table S1). Immunohistochemical analysis revealed that the rAAV2-injected muscles showed much more infiltration of CD4<sup>+</sup> and CD8<sup>+</sup> T lymphocytes in the endomysial space than the rAAV8-injected muscles did (Figure 3a). mRNA levels of TGF- $\beta$ 1 and IL-6 (representative markers of inflammation) in the rAAV-injected muscles were standardized with the  $\beta$ -gal expression. rAAV2-injected muscles had higher TGF- $\beta$ 1 and IL-6 expression than rAAV8-transduced muscles (Supplementary Figure S3). We also examined humoral immune responses against the rAAV particles in the sera of rAAV-injected dogs. The levels of serum IgG in reaction to rAAV2 or rAAV8 gradually increased with time in both serotypes (Figure 3b). These results suggest

**Table 1 Summary of gene transduction experiments**

Dog ID	Sex	Age <sup>a</sup>	BW <sup>b</sup>	rAAV serotype	Transgene	Route	Muscle	Vector dose <sup>c</sup>	Transgene expression <sup>d</sup>			Cellular infiltration <sup>e</sup>		
									2 weeks	4 weeks	8 weeks	2 weeks	4 weeks	8 weeks
2201MN	M	10	4.5	2	lacZ	i.m.	TA, ECR	1 × 10 <sup>11</sup>	–	–	–	–	++	
3004MN	M	5	2.8	2	lacZ	i.m.	TA, ECR	1 × 10 <sup>11</sup>	±	–	–	+	±	
3007FN	F	5	2.5	2	lacZ	i.m.	TA, ECR	1 × 10 <sup>11</sup>	±	±	–	++	++	
2204FN	F	10	2.5	2	lacZ	i.m.	TA, ECR	1 × 10 <sup>12</sup>	–	–	–	+	++	
2801FN	F	10	5.2	2	lacZ	i.m.	TA, ECR	1 × 10 <sup>12</sup>	+	–	–	+	++	
2901MN	M	6	2.8	2	lacZ	i.m.	TA, ECR	1 × 10 <sup>12</sup>	–	–	–	±		
7M48	M	7	3.3	2	lacZ	i.m.	TA, ECR	1 × 10 <sup>12</sup>	–	–	–	+		
2206FN	F	10	3.0	2	lacZ	i.m.	TA, ECR	1 × 10 <sup>13</sup>	±	±	–	+	++	
2205MN	M	10	4.2	8	lacZ	i.m.	TA, ECR	1 × 10 <sup>11</sup>	++	±	–	–	++	
2905MN	M	6	2.8	8	lacZ	i.m.	TA, ECR	1 × 10 <sup>11</sup>	±	–	–	–		
NL52F	F	10	3.5	8	lacZ	i.m.	TA, ECR	1 × 10 <sup>12</sup>	+++	–	–	±		
2106FN	F	6	3.2	8	lacZ	i.m.	TA, ECR	1 × 10 <sup>12</sup>	+++	–	–	–	++	
7M49	F	6	3.2	8	lacZ	i.m.	TA, ECR	1 × 10 <sup>12</sup>	–	±	–	–	++	±
2109FMN	M	7	3.3	8	lacZ	i.m.	TA, ECR	1 × 10 <sup>12</sup>	+++	–	–	–		
2903MN	M	6	3.2	8	lacZ	i.m.	TA, ECR	1 × 10 <sup>12</sup>	+++	–	–	±		
2209MN	M	10	4.3	8	lacZ	i.m.	TA, ECR	1 × 10 <sup>13</sup>	+++	±	–	±	+++	
2309FA	F	6	3.2	8	M3	i.m.	TA, ECR	1 × 10 <sup>12</sup>	±	+	–	–		
LH49F	F	8	3.3	8	lacZ	i.v.		1 × 10 <sup>14</sup>	+++	–	–	+		
3805MN	M	6	3.5	8	lacZ	i.v.		1 × 10 <sup>14</sup>	–	+++	+	–	+	+
2704FA	F	8	3.6	8	M3	i.v.		1 × 10 <sup>14</sup>	+	+++	–	–		
4001MA	M	6	3.2	8	M3	i.v.		1 × 10 <sup>14</sup>	–	+++	+	–		

BW, body weight; F, female; M, male.

<sup>a</sup>Age at injection (weeks). <sup>b</sup>BW at injection (kg). <sup>c</sup>Vectors (vg/ml) were intramuscularly (i.m.) injected into extensor carpi radiolis (ECR) (1 ml) and tibialis anterior (TA) (2 ml) on both sides. Vectors were also intravenously (i.v.) injected into the lateral saphenous vein (vg/kg/limb) by using limb perfusion method. <sup>d</sup> $\beta$ -Gal or microdystrophin-positive fibers per 3,000 fibers: –, 0; ±, <100; +, <300; ++, <1,000; +++, >1,000. <sup>e</sup>Infiltrating cells: –, not detected; ±, a few; +, moderate; ++, extensive.

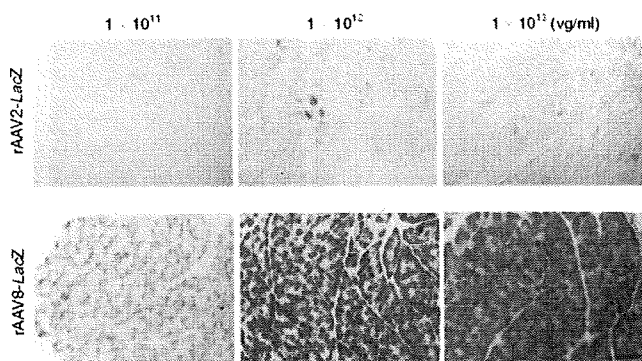


**Figure 1** Canine skeletal muscles stained for  $\beta$ -galactosidase. Two milliliters of rAAV2-*lacZ* or rAAV8-*lacZ* ( $1 \times 10^{11}$ – $10^{13}$  vg/ml) were injected intramuscularly into the tibialis anterior (TA) muscle of normal dogs ( $n = 16$ ) under ultrasonographic guidance. The muscles were biopsied 2 weeks after the injection. Upper: rAAV2-*lacZ*-injected TA muscles, Lower: rAAV8-*lacZ*-injected TA muscles. Bar = 200  $\mu$ m.

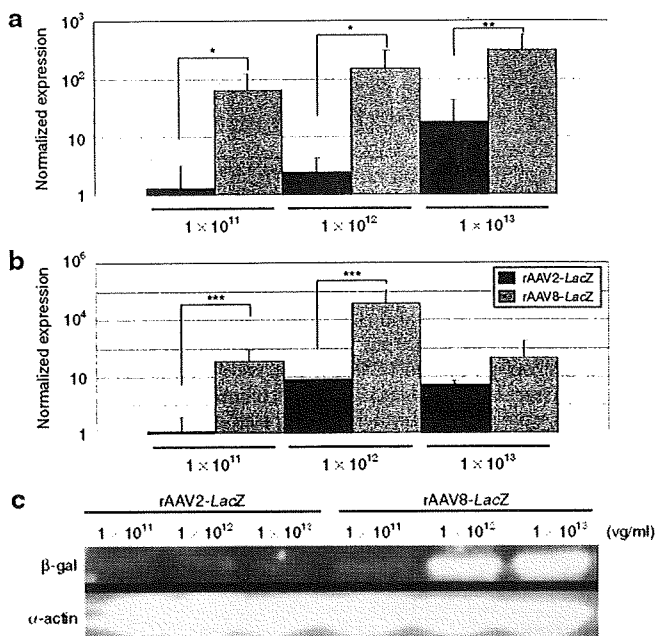


**Figure 2** Quantification of viral vector genome, mRNA, and transgene expression. **(a)** Relative quantification of genomic PCR for rAAV2-*lacZ*-injected muscle (black bars) or rAAV8-*lacZ*-injected muscle (gray bars). DNA samples were extracted from the TA muscles. \* $P < 0.05$ . \*\* $P < 0.01$ . Error bars represent 2 SD. **(b)** Relative quantification showed more extensive  $\beta$ -gal mRNA expression caused by rAAV8-*lacZ* (gray bars) as compared to that caused by rAAV2-*lacZ* (black bars). 18S rRNA was used for an internal control. \*\*\* $P < 0.05$ . Error bars represent 2 SD. **(c)** Western blots of  $\beta$ -gal protein (120 kDa) and  $\alpha$ -actin (42 kDa); the  $\beta$ -gal signal was normalized to  $\alpha$ -actin for comparison.

that cellular and humoral immune responses are elicited in both rAAV2- and rAAV8-transduced muscles.

### Bone marrow-derived DC reactions to rAAV2 and rAAV8

We next cultured bone marrow-derived DCs to investigate their response to rAAV injection in dogs. Flow cytometric analyses of these cells at 7 days of culture revealed marked expressions of CD11c and MHC class II molecules on the

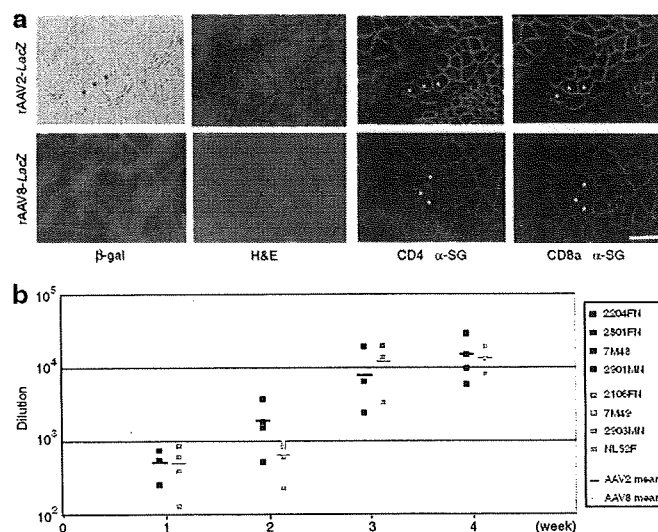


**Figure 3** Immune response to rAAV. **(a)** Lymphocyte infiltration after rAAV transduction. Muscles were biopsied 2 weeks after rAAV2- or rAAV8-*lacZ* injection ( $2 \times 10^{12}$  vg/muscle). Serial cross-sections were stained with  $\beta$ -gal and H&E, and were immunohistochemically stained with antibodies against canine CD4, CD8a (Alexa 568, red), and  $\alpha$ -sarcoglycan ( $\alpha$ -SG, Alexa 488, green). Upper: rAAV2-*lacZ*-injected TA muscle; lower: rAAV8-*lacZ*-injected TA muscle. Bar = 100  $\mu$ m. **(b)** Humoral immune responses to rAAV capsid in dogs. Serum was collected weekly from rAAV2- or rAAV8-*lacZ*-injected dogs and analyzed for the presence of IgG antibody against the rAAV2 or rAAV8 capsid. The data represent dilution rates with 50% reactivity of anti-rAAV2 (black boxes) and anti-rAAV8 (gray boxes) capsid antibodies. The mean reconstitution values are shown as straight lines. Each symbol represents an individual dog that was injected with rAAV at  $2 \times 10^{12}$  vg/muscle.

surface (Figure 4a,b). The DCs were cultured with the rAAV-*luciferase* of either serotype 2 or 8 for 48 hours to evaluate transduction efficiency, or cultured with rAAV-*lacZ* for 4 hours to investigate kinetic changes in mRNA. The luciferase assay showed that the transduction efficiency of rAAV2-*luciferase* in DCs was approximately two times that of rAAV8-*luciferase* (Figure 4c). mRNA levels of MyD88 and costimulating factors, such as CD80, CD86, and type I interferon (interferon- $\beta$ , IFN- $\beta$ ) were elevated in both conditions (Figure 4d), suggesting that rAAV8 also induces a considerable degree of innate immune response in dog skeletal muscles. Although rAAV2-transduced DCs showed higher IFN- $\beta$  expression than rAAV8-transduced DCs, the differences between the effects of rAAV2 and rAAV8 on the mRNA levels of MyD88, CD80, CD86, and IFN- $\beta$  were not statistically significant.

### Successful microdystrophin gene transfer with rAAV8 into dystrophic dogs

Dystrophin expression in normal skeletal muscle is localized on the sarcolemma, whereas it is totally absent in CXMD<sub>1</sub> dogs (Supplementary Figure S4a,b). Microdystrophin expression in the rAAV8-injected skeletal muscle of CXMD<sub>1</sub> dogs was maintained, even in the absence of any immunosuppressive therapy, for at least 4 weeks after the injection (Table 1). Previously, we had shown that microdystrophin expression of ca 20% was sufficient to achieve functional recovery in mdx mice<sup>6</sup>. However, the amount of the expression in intramuscularly injected muscles

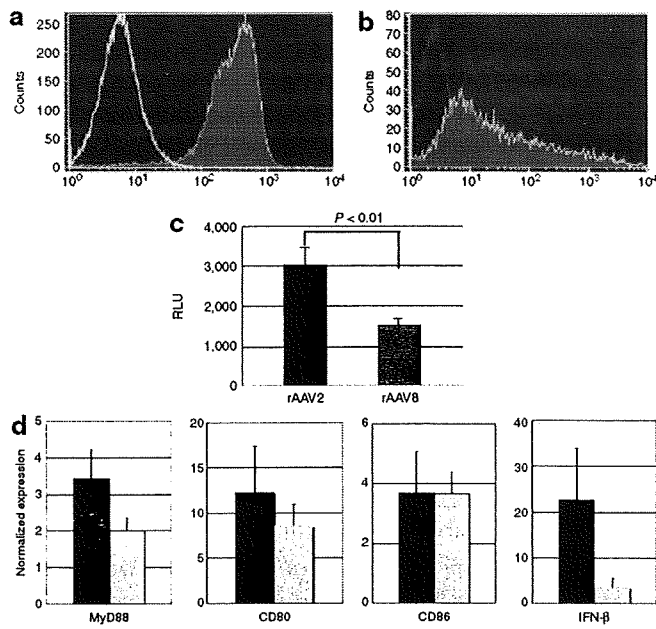


**Figure 4 Responses of dendritic cells (DCs) to rAAV in dogs.** Bone marrow-derived DCs were obtained from the humerus bones of dogs and cultured in RPMI (10% FCS, p/s) for 7 days with canine GM-CSF and IL-4. **(a)** Flow cytometric analysis of cell surface molecules on day 7. The cells were stained with PE-conjugated CD11c antibody and isotype control. **(b)** DCs were stained with FITC-conjugated MHC Class II antibody and isotype control. **(c)** DCs were transduced with rAAV-luciferase ( $1 \times 10^6$ vg/cell) for 48 hours. To analyze luciferase expression relating to the use of rAAV2 or rAAV8, relative light unit (RLU) ratios were measured.  $*P < 0.01$ . Error bars represent s.e.m.,  $n = 8$ . **(d)** DCs were transduced with  $1 \times 10^6$ vg/cell of rAAV2 (black bars) or rAAV8-lacZ (gray bars) for 4 hours, and mRNA levels of MyD88, CD80, CD86, and IFN-β were analyzed. Untransduced cells were used as a control to demonstrate the relative value of expression. The results are representative of two independent experiments. Error bars represent s.e.m.,  $n = 3$ .

seemed to be insufficient to produce the expected functional recovery (Supplementary Figure S4c).

For more efficient gene delivery by rAAV8, we tried a limb perfusion method in the hind limb through the lateral saphenous vein, in an attempt to prevent muscle damage due to direct injection and to bypass immune activation through DCs in the injected muscle. We had observed highly efficient β-gal expression in nearly all the muscles of the distal hind limb at 2 weeks after a single injection (Table 1, Figure 5a). We then injected rAAV8-M3 into the hind limbs of CXMD<sub>1</sub> dogs, using the same method (Table 1). The induction of microdystrophin expression in the muscle at 4 weeks after intravascular injection was more efficient and free of noticeable immune response as compared to intramuscularly injected muscle (Figure 5b, Supplementary Figure S4d). These results suggest that the intravascular method is superior to the intramuscular method of administration. Although microdystrophin expression persisted at 8 weeks after injection of rAAV8-M3, the number of microdystrophin-positive cells at this time point was lower than in the muscles that were sampled at 4 weeks after injection. It is clear, therefore, that long-term microdystrophin expression can be obtained by the limb perfusion method, but that the expression does not last at the same level over a period of weeks. The same phenomenon was

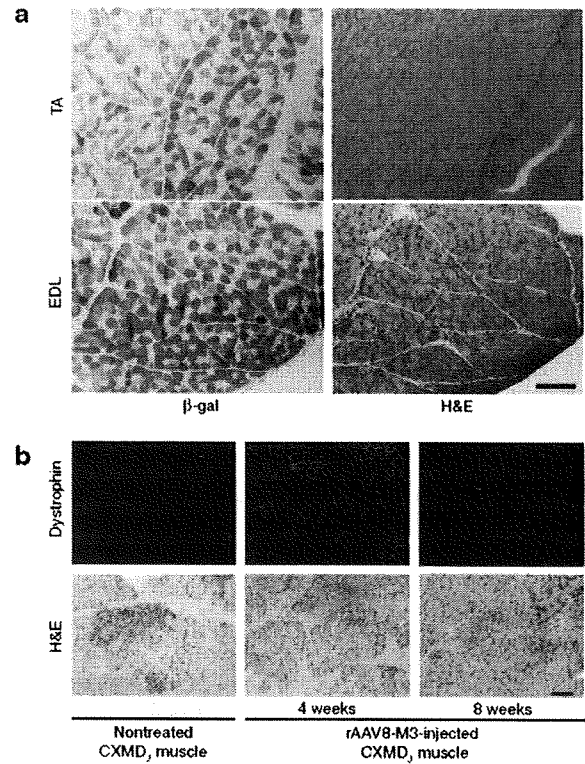


**Figure 5 rAAV8-mediated muscle transduction using the limb perfusion method.** **(a)** Transduction of normal dog with rAAV8-lacZ, using the limb perfusion method. Muscles were biopsied 2 weeks after the injection and stained with β-gal and H&E. TA, tibialis anterior, EDL, extensor digitorum longus. Bar = 200 μm. **(b)** Transduction of canine X-linked muscular dystrophy in Japan (CXMD) dog with rAAV8-M3. Muscles of CXMD<sub>1</sub> dogs were biopsied 4 and 8 weeks after limb perfusion with rAAV8-M3. Samples were immunohistochemically stained with anti-dystrophin antibody (dys2, NCL). Left: nontreated CXMD<sub>1</sub> muscle. Middle and right: muscles injected with rAAV-M3 using limb perfusion method, examined at 4 or 8 weeks after the transduction. Bar = 100 μm.

observed in rAAV8-lacZ-transduced muscles (Supplementary Figure S5).

**DISCUSSION**

In this article, we present evidence that the transfer of rAAV8-lacZ to canine skeletal muscles produces higher transgene expression with less lymphocyte proliferation than rAAV2-lacZ does, at 2 weeks after injection. Given the advantages of rAAV8, the administration of rAAV8-M3 by limb perfusion produced extensive transgene expression in the distal limb muscles of CXMD<sub>1</sub> dogs without obvious immune responses for as long as 8 weeks after injection. However, transgene expression in the rAAV8-transduced muscles attenuated in the absence of an immunosuppressive regimen over the course of observation. In addition, humoral immune responses were elicited by both rAAV2 and rAAV8. mRNA levels of MyD88 and costimulating factors such as CD80, CD86, and type I interferon (interferon-β) were elevated in both rAAV2- and rAAV8-transduced DCs *in vitro*.

In our previous study, we had demonstrated extensive lymphocyte-mediated immune responses to rAAV2-lacZ after direct intramuscular injection into dogs, in contrast to the reported successful delivery of the same viral construct into mouse skeletal

muscle.<sup>8</sup> The fact that the promoter-deleted rAAV2 caused fewer cytotoxic cellular responses suggested that the massive destruction of transduced muscle cells might be the result of cellular immunity against the transgene product. In this study, there was extensive expression of  $\beta$ -gal in rAAV8-*lacZ*-injected canine muscles even in the absence of any immunosuppressive treatments (Figure 1), while the rAAV2-*lacZ*-injected muscles showed minimal  $\beta$ -gal expression with considerable inflammatory infiltration. If the transgene product were the main inducer of immune responses, lymphocyte activation would be correlated with transduction efficiency; however, this is not the case based on our results relating to the vector genome, mRNA expression level, and protein delivered through either rAAV2 or rAAV8 (Figure 2). These data suggested that the rAAV particle is associated with potent immunogenicity. Besides,  $\beta$ -gal expression disappeared 4 weeks after injection in the rAAV8-injected muscle as in the rAAV2-transduced muscles (Supplementary Figure S2). To investigate whether AAV itself has immunogenicity properties, we further characterized the immune responses caused by rAAV2 or rAAV8.

Immunohistochemical analysis revealed that the rAAV2-injected muscles showed higher rates of infiltration of CD4<sup>+</sup> and CD8<sup>+</sup> T lymphocytes in the endomysium than rAAV8-injected muscles did (Figure 3a). Considering the stringent immunogenicity of *lacZ* gene expression, we normalized the activity of TGF- $\beta$ 1 and IL-6 by *lacZ* expression to exclude the effect of transgene products (Supplementary Figure S3a). The total activity of TGF- $\beta$ 1 and IL-6 in the rAAV8-injected muscles was higher than that in rAAV2-injected muscles (Supplementary Figure S3b). As a result, rAAV2 induced a stronger cellular immune response than rAAV8 did. To investigate the humoral immune response, we quantitated neutralizing antibodies against rAAV particles in the sera of rAAV-injected dogs (Figure 3b). Antibodies against AAV2 and AAV8 capsids were below the detectable level before the injection and were elevated with time after the injection. Because the dogs were bred in a specific pathogen-free facility and not vaccinated, we assume that the elevation of antibody levels was not caused by anamnestic reaction.

Recently, Li *et al.*<sup>10</sup> reported that the AAV2 capsid can induce a cellular immune response through MHC class I antigen presentation with a cross-presentation pathway, and the effects of rAAV2 on human DCs have been described.<sup>10,13</sup> In contrast, other serotypes such as rAAV8 induced less T-cell activation.<sup>11,14</sup> Plasmacytoid DCs are critically important in innate immunity because of their unsurpassed ability to present adenoviral antigens to T-cells for the generation of primary cellular and humoral immune responses.<sup>15-17</sup> The response of DCs against rAAV in dogs was yet to be elucidated. We prepared bone marrow-derived DCs to investigate rAAV-mediated transduction of DCs. The difference between rAAV2 and rAAV8 in respect of the transduction rate of DCs *in vitro* was no greater than the difference in distinct  $\beta$ -gal expressions *in vivo* (Figure 2,4c). Quantitative analysis of mRNA of the transduced DCs by RT-PCR revealed that both rAAV2 and rAAV8 upregulated the expression of costimulating factors, with no significant difference between mRNA levels in rAAV2- and rAAV8-transduced cells. Therefore, both rAAV2 and rAAV8 may activate innate immunity in the context of extensive muscle transduction. Whereas AAV capsids cause immune

response, transgene products may play adjuvant roles in the immunity to the AAV capsids.<sup>18</sup>

rAAV8 encoding the human *microdystrophin* gene was also intramuscularly injected into the skeletal muscles of CXMD<sub>1</sub> dogs. rAAV8-mediated gene expression without any immunosuppression was confirmed over a period of 8 weeks after the injection, whereas there was much less transduction with the use of rAAV2 (data not shown). rAAV8-mediated transduction was also expected to provide effective intravenous delivery.<sup>12</sup> In this context, the venous system is an attractive route for limb perfusion administration because it is a direct channel to multiple muscles of the limb. Moreover, veins are easier to access through the skin and there is less potential for muscle damage during injection. By using the limb perfusion method, we could reach nearly all the muscles of the lower limb, held transiently isolated by a tourniquet around the thigh. Limb perfusion administration could possibly have the potential to bypass the DC recognition caused by intramuscular injection. We intravenously injected rAAV8-*lacZ* into the hind limbs of normal dogs and rAAV8-*M3* into the hind limbs of CXMD<sub>1</sub> dogs, and obtained more extensive expression of  $\beta$ -gal or microdystrophin than by intramuscular injection. Interestingly, the inflammatory response was not significant in the intravenously injected muscles, although no immune suppression was attempted. We think that one reason rAAV8-*M3* resulted in better expression than rAAV8-*lacZ* is that the immunogenicity of *M3* is lower than that of *lacZ*. Although microdystrophin expression was lower at 8 weeks after the transduction with the limb perfusion, cellular infiltration was not significant.

In the future, systemic delivery of rAAV8-*microdystrophin* could ameliorate the symptoms of DMD patients. Even though portal vein injection of rAAV2-*FLX* into hemophilia B dogs produced long-term expression, a clinical study failed to demonstrate long-term expression in humans.<sup>19,20</sup> In advance of future clinical trials, several studies are required to confirm safety. Sequential peripheral blood monitoring showed no severe adverse events, including liver dysfunction, during 8 weeks (data not shown). We are now developing a systemic delivery strategy with a muscle-specific promoter. It is also necessary to improve vector constructs or regulate immune reaction against transgene products. Recently, Wang *et al.* reported sustained AAV6-mediated human microdystrophin expression in dystrophic dogs for 30 weeks, using combined immunosuppressive therapy of Cyclosporin, Mycophenolate Mofetil, and anti-thymocyte globulin.<sup>9</sup> In this study with rAAV8-*M3*, we confirmed effective transduction into dog skeletal muscle for 4 weeks without immunosuppressive therapy. However, considering the fact that not only rAAV2 but also rAAV8 induced activation of DCs *in vitro*, immunological modulation would be required for sufficient long-term expression. A novel protocol with systemic or localized immunosuppression using immunosuppressive drugs or local immunosuppression with an IFN- $\alpha$  or - $\beta$  blockade could help avoid host immune reaction.

In summary, we achieved successful rAAV8-mediated muscle transduction in wild-type dogs as well as in dystrophic dogs by using the limb perfusion method of administration. Also, by manipulating bone marrow-derived DCs, we observed the probable contribution of antigen-presenting cells to the immune response against rAAV8-mediated gene therapy. Although the

cellular responses against rAAV8 were not significant *in vivo*, this DC activation may possibly be involved in limiting long-term transduction when the limb perfusion method is used. The limb perfusion transduction protocol with improved AAV constructs or immune modulation would further enhance rAAV8-mediated transduction strategy and lead to therapeutic benefits.

## MATERIALS AND METHODS

**Animals.** Five- to ten-week-old male and female wild-type dogs obtained from the Beagle-based CXMD<sub>1</sub> breeding colony at the National Center of Neurology and Psychiatry (Tokyo, Japan) were used for the *lacZ* gene transduction.<sup>3</sup> Six- to eight-week-old CXMD<sub>1</sub> dogs were used for *microdystrophin* gene transduction. All the animals were cared for and treated in accordance with the guidelines approved by the Ethics Committee for Treatment of Laboratory Animals at National Center of Neurology and Psychiatry, where the three fundamental principles of replacement, reduction, and refinement are also considered. Dogs were not vaccinated to avoid the immune responses to vaccination.

**Construction of proviral plasmid and recombinant AAV vector production.** The AAV2 vector proviral plasmids harboring the *lacZ* or *luciferase* gene with a CMV promoter and SV40 late-gene polyadenylation sequence were propagated.<sup>8</sup> As a therapeutic gene for DMD, the human *microdystrophin* gene, *M3*, was used under the control of the CMV promoter and a bovine growth hormone polyadenylation sequence.<sup>21</sup> The vector genome was packaged into the AAV2 capsid or pseudotyped AAV8 capsid in HEK293 cells. A large-scale cell culture method with an active gassing system was used for transfection.<sup>22</sup> The vector production process involved triple transfection of a proviral plasmid, an AAV helper plasmid pAAV-RC (Stratagene, La Jolla, CA) or p5E18-VD2/8, and an adenovirus helper plasmid pHelper (Stratagene).<sup>21</sup> All the viral particles were purified by CsCl gradient centrifugation. The viral titers were determined by quantitative PCR using SYBR-green detection of PCR products in real time with the MyiQ single-color detection system (Bio-Rad, Hercules, CA) and the following primer sets: for AAV-*lacZ*, *lacZ*-Q60: forward primer 5'-TTATCAGCCGGAAAACCTACCG-3', and reverse primer 5'-AGCCAGTTTACCCGCTCTGCTA-3'; for AAV-*microdystrophin*: forward primer 5'-CCAAAAGAAAAAGGATCCACAA-3', and reverse primer 5'-TTCCAAATCAAACCAAGAGTCA-3'; and for AAV-*luciferase*: forward primer 5'-GATACGCTGCTTAAATGCCTTT-3', and reverse primer 5'-GTTGCGTCAGCAAACACAGT-3'.

**Direct administration of rAAVs into normal and dystrophic skeletal muscle.** Experimental dogs ( $n = 16$ ) were sedated with isoflurane by mask inhalation and intubated. Anesthesia was maintained with 2–4% isoflurane. Two milliliters of rAAV2-*lacZ* or rAAV8-*lacZ* ( $1 \times 10^{11}$ – $10^{13}$  vg/ml) were injected intramuscularly into the tibialis anterior muscles and 1 ml into the extensor carpi radialis muscles of the normal dogs under ultrasonographic guidance. rAAV8-*M3* ( $1 \times 10^{12}$  vg/ml) was intramuscularly injected at a volume of 2 ml into the tibialis anterior muscles and 1 ml into the extensor carpi radialis muscles of a CXMD<sub>1</sub> dog.

**Intravenous delivery of rAAVs into the limb veins of dogs.** Intravenous injection was administered as described elsewhere.<sup>12</sup> Briefly, a blood pressure cuff was applied just above the knee of an anesthetized normal dog. A 24-gauge intravenous catheter was inserted into the lateral saphenous vein, connected to a three-way stopcock, and flushed with saline. With the blood pressure cuff inflated to over 300 mm Hg, saline (2.6 ml/kg) containing papaverine (0.44 mg/kg, Sigma-Aldrich, St Louis, MO) and heparin (16 U/kg) was injected by hand over 10 seconds. The three-way stopcock was connected to a syringe containing rAAV8-*lacZ* ( $1 \times 10^{14}$  vg/kg, 3.8 ml/kg). The syringe was placed in a PHD 2000 syringe pump (Harvard Apparatus, Edenbridge, UK). Five minutes after the

papaverine/heparin injection, the rAAV8-*lacZ* was injected at a rate of 0.6 ml/second. Two minutes after the rAAV injection, the blood pressure cuff was released and the catheter was removed. The CXMD<sub>1</sub> dogs were injected with rAAV8-*M3* using the same method.

**Sampling of transduced muscles.** Either the muscles of the transduced dogs were biopsied or the animals were killed at 2, 4, and 8 weeks after the injection. We sampled tibialis anterior and extensor carpi radialis muscles on both sides in the intramuscularly transduced dog. In the case of the limb perfusion study, tibialis anterior or extensor digitorum longus muscle of the injected side of the leg was sampled. For biopsy and necropsy, the individual muscle was cropped tendon-to-tendon, divided into several pieces, and immediately frozen in liquid nitrogen-cooled isopentane. Two to eight blocks were sampled from the transduced muscle. We analyzed at least 30 sections from the blocks to observe the general representation.

**Histological analysis.** Transverse cryosections (10  $\mu$ m) from the rAAV-*lacZ*-injected muscles were stained with hematoxylin and eosin or 5-bromo-4-chloro-3-indolyl- $\beta$ -D-galactopyranoside.<sup>23</sup> Eight-micrometer-thick cryosections from the rAAV-*M3*-injected muscles were immunohistochemically stained as described.<sup>24</sup> Briefly, the cryosections were fixed by immersion in cold acetone at  $-20^{\circ}\text{C}$ . Fixed frozen sections were blocked in 5% goat serum in phosphate-buffered saline at room temperature and incubated with mouse monoclonal anti-dystrophin C-terminal antibody (NCL-dys2, Novocastra, Newcastle upon Tyne, UK). The signal was visualized with an Alexa 568-conjugated anti-mouse IgG. Fluorescent signals were observed using a confocal laser scanning microscope (Leica TCS SP, Leica, Heidelberg, Germany). Immunohistochemical analyses were performed with mouse monoclonal antibodies against canine CD4 (CA13.1E4, Serotec, Oxford, UK), canine CD8a (CA9.JD3, Serotec), and double-stained with rabbit polyclonal antibody against  $\alpha$ -sarcoglycan.<sup>25</sup> The signal was visualized with an Alexa 568-conjugated anti-mouse IgG, and 488-conjugated anti-rabbit IgG.

**Detection of AAV genomes.** Total DNA was extracted from muscle cryosections. Cryosections were homogenized using a Multi-beads shocker (Yasui Kikai, Osaka, Japan), and extracted using a Wizard SV Genomic DNA purification system (Promega, Madison, WI). The rAAV genome was detected by relative quantitative PCR using SYBR-green detection of PCR products in real time with a primer set of *lacZ*-Q60. For an internal control, forward primer, 5'-GAACACGCGTTAATAAGGCAATCA-3', and reverse primer, 5'-CTGACATTCATCGCATCTTTGACA-3', directed to an ultra-conserved region, were used.<sup>26</sup>

**Real-time RT-PCR.** Total RNA was isolated from cryosections using a Multi-beads shocker (Yasui Kikai), and RNeasy Fibrous Tissue Mini kit (Qiagen, Hilden, Germany), and first-strand cDNA was synthesized using a QuantiTect Reverse Transcription kit (Qiagen). mRNA was detected using primer sets of *lacZ*-Q60, forward primer 5'-TGATGGCTA CTGCTTCCCTAC-3' and reverse primer 5'-GAGATTTTGCCGA GGATGTACT-3' for IL-6, and forward primer 5'-CAAGGATCTGGG TGGAAAGTGGGA-3' and reverse primer, 5'-CCAGGACCTTGCTGTA CTGCGGT-3' for TGF- $\beta$ 1. For an internal control, a primer set of 18S rRNA (Ambion, Foster City, CA) was used.

**Western blot analysis.** Muscle cryosections were homogenized with four volumes of sample buffer (10% SDS, 70 mmol/l Tris-HCl, 10 mmol/l EDTA, and 5%  $\beta$ -mercaptoethanol). The samples were boiled for 5 minutes and centrifuged at 14,500 rpm for 15 minutes. Protein samples (30  $\mu$ g per lane) were electrophoresed on a 7.5% polyacrylamide gel (Bio-Rad). The membranes were incubated with a 1:1,000 dilution of the primary antibody for detecting 120 kDa *lacZ* protein (rabbit anti- $\beta$ -galactosidase IgG fraction, Molecular Probes, Eugene, OR) or 42 kDa  $\alpha$ -actin (mouse anti- $\alpha$ -sarcomeric actin IgM, Sigma-Aldrich). Anti-rabbit IgG peroxidase F(ab')

(GE Healthcare, Buckinghamshire, UK), or peroxidase-conjugated donkey anti-mouse IgM (Jackson ImmunoResearch Laboratories, West Grove, PA) was used for ECL immunodetection (GE Healthcare). Quantification of LacZ protein was performed using a specialized software (ImageJ, US National Institutes of Health, Bethesda, MD).

**ELISA for anti-canine AAV IgG.** A microtiter plate (MS-8596F, Sumitomo Bakelite, Tokyo, Japan) was precoated with promoter-deleted rAAV2 or rAAV8 ( $2 \times 10^9$  genomes/well) and blocked with a blocking buffer (Block Ace, DS Pharma Biomedical, Osaka, Japan). The plate was incubated for 2 hours at room temperature with the sera from rAAV-transduced dogs, followed by a 1:5,000 dilution of peroxidase-conjugated rabbit anti-dog IgG (Sigma-Aldrich) for 1 hour. Color was visualized using a peroxidase substrate system (TMBZ, ML-1120T, Sumitomo Bakelite). Reactivity was detected at a wave-length of 450 nm with a reference at 570 nm, using an APPLISKAN Multimode Reader (Thermo Fisher Scientific, East Greenbush, NY).

**Bone marrow aspiration and preparation of DCs.** After the dogs were anesthetized with thiopental and isoflurane, ~0.5 ml of bone marrow was obtained from each humerus by aspiration with a syringe containing 2 ml of 16 mmol/l EDTA-2Na PBS. Bone marrow-derived DCs were generated as described.<sup>15</sup> Mononuclear cells were isolated by density centrifugation using Histopaque-1077 (Sigma-Aldrich). Cells were suspended in RPMI-1640 culture medium (Invitrogen, Carlsbad, CA) supplemented with 10% fetal bovine serum (MP Biomedicals, Aurora, OH) and 1% penicillin-streptomycin (Sigma-Aldrich), and cultured at 37°C in a humidified 5% CO<sub>2</sub>-containing atmosphere. Recombinant canine GM-CSF (25 ng/ml, R&D Systems, Minneapolis, MN) and canine IL-4 (12.5 ng/ml, R&D Systems) were added to the culture medium. On days 3 and 5 of the culture, 60% of the medium volume was changed. On day 7 of the culture, loosely adherent cells were collected and used for fluorescence-activated cell analysis. A FACS Vantage system (Becton Dickinson, Franklin Lakes, NJ) was used for flow cytometry event collection. For the purpose of examining the infectious rate of rAAV, cells were cultured for 48 hours with rAAV2- or 8-*luciferase*. The luciferase activity of rAAV2- or rAAV8-*luciferase* co-cultured cells was estimated using an APPLISKAN Multimode Reader (Thermo Fisher Scientific). Total RNA was isolated using an RNeasy Fibrous Tissue Mini kit (Qiagen), and QuantiTect Reverse Transcription kit (Qiagen). mRNA of cytokines were analyzed using the primer set, forward primer 5'-GAGGAGATGGGCTTCGAGTA-3' and reverse primer 5'-GTTCCACCAACACGTCGTC-3' for MyD88; forward primer 5'-GCATCATCCAGGTGAACAAG-3' and reverse primer 5'-AAGTCAGCAAAGGTGCGATT-3' for CD80; forward primer 5'-AGGTTACCCAGAACCCAAAGG-3' and reverse primer, 5'-TTGCAGGACACAGAAGATGC-3' for CD86; and forward primer 5'-ATTGCCTCAAGGACAGGATAAA-3' and reverse primer 5'-TTGACGTCCTCCAGGATATCT-3' for IFN- $\beta$ . mRNA levels of MyD88, CD80, CD86, and IFN- $\beta$  in DCs were normalized with a house keeping gene, 18s rRNA. The mRNA levels in the transduced cells were presented as ratios relative to the sample obtained from the untransduced DCs.

**Statistical analysis.** Statistical significance was determined on the basis of an unpaired, two-tailed Student's *t*-test using specialized software (Statview; SAS Institute, Cary, NC). A *P* value of <0.05 was considered significant.

#### SUPPLEMENTARY MATERIAL

**Figure S1.** Histological findings with incisional and nonincisional injection under ultrasonographic guidance.

**Figure S2.**  $\beta$ -gal expression 4 weeks after injection.

**Figure S3.** Levels of mRNA were investigated using rAAV-injected muscles.

**Figure S4.** Intramuscular injection of rAAV8-M3 into CXMD,

**Figure S5.** Long-term  $\beta$ -gal expression using limb perfusion injection.

**Table S1.** Protein expression analyzed with ImageJ.

#### ACKNOWLEDGMENTS

We thank James M. Wilson for providing p5E18-VD2/8. We also thank Akinori Nakamura, Hiroyuki Nakai, Yuko Nitahara-Kasahara, and Toshimasa Aranami for technical advice and helpful discussions; Kazue Kinoshita for AAV preparation; Ryoko Nakagawa for technical assistance; Satoru Masuda for FACS analysis; and Hideki Kita, Shinichi Ichikawa, and other staff members of JAC Co. for their care of the dogs. This work is supported by Grants-in-Aid for Scientific Research on Nervous and Mental Disorders and Health Sciences Research Grants for Research on Human Genome and Gene Therapy from the Ministry of Health, Labor and Welfare of Japan, and a Grant-in-Aid for Scientific Research from the Ministry of Education, Culture, Sports, Science and Technology (MEXT).

#### REFERENCES

- Valentine, BA, Cooper, BJ, de Lahunta, A, O'Quinn, R and Blue, JT (1988). Canine X-linked muscular dystrophy. An animal model of Duchenne muscular dystrophy: clinical studies. *J Neurol Sci* **88**: 69–81.
- Sharp, NJ, Komegay, IN, Van Camp, SD, Herbstreith, MH, Secore, SL, Kettle, S *et al.* (1992). An error in dystrophin mRNA processing in golden retriever muscular dystrophy, an animal homologue of Duchenne muscular dystrophy. *Genomics* **13**: 115–121.
- Shimatsu, Y, Yoshimura, M, Yuasa, K, Urasawa, N, Tomohiro, M, Nakura, M *et al.* (2005). Major clinical and histopathological characteristics of canine X-linked muscular dystrophy in Japan, CXMD. *Acta Myol* **24**: 145–154.
- Nakai, H, Fuess, S, Storm, TA, Muramatsu, S, Nara, Y and Kay, MA (2005). Unrestricted hepatocyte transduction with adeno-associated virus serotype 8 vectors in mice. *J Virol* **79**: 214–224.
- Wang, Z, Zhu, T, Qiao, C, Zhou, L, Wang, B, Zhang, J *et al.* (2005). Adeno-associated virus serotype 8 efficiently delivers genes to muscle and heart. *Nat Biotechnol* **23**: 321–328.
- Yoshimura, M, Sakamoto, M, Ikemoto, M, Mochizuki, Y, Yuasa, K, Miyagoe-Suzuki, Y *et al.* (2004). AAV vector-mediated microdystrophin expression in a relatively small percentage of mdx myofibers improved the mdx phenotype. *Mol Ther* **10**: 821–828.
- Gregorevic, P, Allen, JM, Minami, E, Blankinship, MJ, Haraguchi, M, Meuse, L *et al.* (2006). rAAV6-microdystrophin preserves muscle function and extends lifespan in severely dystrophic mice. *Nat Med* **12**: 787–789.
- Yuasa, K, Yoshimura, M, Urasawa, N, Ohshima, S, Howell, JM, Nakamura, A *et al.* (2007). Injection of a recombinant AAV serotype 2 into canine skeletal muscles evokes strong immune responses against transgene products. *Gene Ther* **14**: 1249–1260.
- Wang, Z, Kuhr, CS, Allen, JM, Blankinship, M, Gregorevic, P, Chamberlain, JS *et al.* (2007). Sustained AAV-mediated dystrophin expression in a canine model of Duchenne muscular dystrophy with a brief course of immunosuppression. *Mol Ther* **15**: 1160–1166.
- Li, C, Hirsch, M, Asokan, A, Zeithaml, B, Ma, H, Kafri, T *et al.* (2007). Adeno-associated virus type 2 (AAV2) capsid-specific cytotoxic T lymphocytes eliminate only vector-transduced cells coexpressing the AAV2 capsid *in vivo*. *J Virol* **81**: 7540–7547.
- Vandenbergh, LH, Wang, L, Somanathan, S, Zhi, Y, Figueredo, J, Calcedo, R *et al.* (2006). Heparin binding directs activation of T cells against adeno-associated virus serotype 2 capsid. *Nat Med* **12**: 967–971.
- Hagstrom, JE, Hegge, J, Zhang, G, Noble, M, Budker, V, Lewis, DL *et al.* (2004). A facile nonviral method for delivering genes and siRNAs to skeletal muscle of mammalian limbs. *Mol Ther* **10**: 386–398.
- Zhang, Y, Chirmule, N, Gao, G and Wilson, J (2000). CD40 ligand-dependent activation of cytotoxic T lymphocytes by adeno-associated virus vectors *in vivo*: role of immature dendritic cells. *J Virol* **74**: 8003–8010.
- Lin, SW, Hensley, SE, Tatsis, N, Lasaro, MO and Ertl, HC (2007). Recombinant adeno-associated virus vectors induce functionally impaired transgene product-specific CD8 T cells in mice. *J Clin Invest* **117**: 3958–3970.
- Isotani, M, Katsuma, K, Tamura, K, Yamada, M, Yagihara, H, Azakami, D *et al.* (2006). Efficient generation of canine bone marrow-derived dendritic cells. *J Vet Med Sci* **68**: 809–814.
- Zhu, J, Huang, X and Yang, Y (2007). Innate immune response to adenoviral vectors is mediated by both Toll-like receptor-dependent and -independent pathways. *J Virol* **81**: 3170–3180.
- Zhang, Z and Wang, FS (2005). Plasmacytoid dendritic cells act as the most competent cell type in linking antiviral innate and adaptive immune responses. *Cell Mol Immunol* **2**: 411–417.
- Mahadevan, M, Liu, Y, You, C, Luo, R, You, H, Mehta, JL *et al.* (2007). Generation of robust cytotoxic T lymphocytes against prostate specific antigen by transduction of dendritic cells using protein and recombinant adeno-associated virus. *Cancer Immunol Immunother* **56**: 1615–1624.
- Mount, JD, Herzog, RW, Tillson, DM, Goodman, SA, Robinson, N, McClelland, ML *et al.* (2002). Sustained phenotypic correction of hemophilia B dogs with a factor IX null mutation by liver-directed gene therapy. *Blood* **99**: 2670–2676.

20. Manno, CS, Pierce, GF, Arruda, VR, Glader, B, Ragni, M, Rasko, JJ *et al.* (2006). Successful transduction of liver in hemophilia by AAV-Factor IX and limitations imposed by the host immune response. *Nat Med* **12**: 342–347.
21. Sakamoto, M, Yuasa, K, Yoshimura, M, Yokota, T, Ikemoto, T, Suzuki, M *et al.* (2002). Micro-dystrophin cDNA ameliorates dystrophic phenotypes when introduced into mdx mice as a transgene. *Biochem Biophys Res Commun* **293**: 1265–1272.
22. Okada, T, Nomoto, T, Yoshioka, T, Nonaka-Sarukawa, M, Ito, T, Ogura, T *et al.* (2005). Large-scale production of recombinant viruses by use of a large culture vessel with active gassing. *Hum Gene Ther* **16**: 1212–1218.
23. Ishii, A, Hagiwara, Y, Saito, Y, Yamamoto, K, Yuasa, K, Sato, Y *et al.* (1999). Effective adenovirus-mediated gene expression in adult murine skeletal muscle. *Muscle Nerve* **22**: 592–599.
24. Yuasa, K, Sakamoto, M, Miyagoe-Suzuki, Y, Tanouchi, A, Yamamoto, H, Li, J *et al.* (2002). Adeno-associated virus vector-mediated gene transfer into dystrophin-deficient skeletal muscles evokes enhanced immune response against the transgene product. *Gene Ther* **9**: 1576–1588.
25. Araishi, K, Sasaoka, T, Imamura, M, Noguchi, S, Hama, H, Wakabayashi, E *et al.* (1999). Loss of the sarcoglycan complex and sarcospan leads to muscular dystrophy in beta-sarcoglycan-deficient mice. *Hum Mol Genet* **8**: 1589–1598.
26. Sandelin, A, Bailey, P, Bruce, S, Engstrom, PG, Klos, JM, Wasserman, WW *et al.* (2004). Arrays of ultraconserved non-coding regions span the loci of key developmental genes in vertebrate genomes. *BMC Genomics* **5**: 99.



# 先天性筋ジストロフィー(福山型を中心に)

大澤真木子 舟塚 真 東京女子医科大学小児科



## はじめに

筋ジストロフィーは、「筋の壊死と再生を主病変とする進行性の遺伝子異常による疾患」であり、I細胞膜貫通およびその近傍の分子異常である、①ジストロフィン異常症(Duchenne型, Becker型, 中間型), ②サルコグリカン異常症(肢帯型), ③カベオリン異常症(肢帯型), II基底膜とそれを細胞膜に固定する分子の異常である先天性(福山型(FCMD), Walker-Warburg症候群(WWS), 筋・眼・脳病(MEB), メロシン欠損型)とIII核膜分子異常であるEmery-Dreifuss型に分けられる。異常分子が細胞表面に近いほど, 重篤な傾向がある。

先天性であるFCMD, MEB, WWSでは,  $\alpha$ ジストログリカンの異常が関連し, 脳の形成障害と眼症状も伴う。少なくとも6つの遺伝子(FKTN, POMGNT1, POMT1, POMT2, FKRP, LARGE)の変異が関係し<sup>1-3)</sup>, 臨床像には幅がある。フクチン遺伝子(FKTN)は9q31にあり, その産物は, 461アミノ酸(分子量53.7kDa)からなる。FKTN異常でもWWSのような重症例から心筋症のみの軽症例<sup>4,5)</sup>が存在する。FCMDの大部分は, 3kbのDNAの挿入を3'非翻訳領域内に認める共通の祖先由来のancestral haplotype(創始者染色体)を有する。日本人に多く, 頻度は約10万人に1人, 保因者は約80人に1人である。FKTN異常で, 脳表の神経細胞の移動異常で脳形成障害, 筋の脆弱性が生じ, 物理的的刺激により胎生中期以降筋変性過程が進むと推測される。創始者ハプロタイプホモ結合型は, 軽症/典型例に多く, 創始者ハプロタイプとの複合ヘテロ結合型では, 重症が多い傾向がある。全体像概説と急性感染症に伴う一過性筋力低下, 心機能の管理, 骨格筋の進行性病

変に伴う呼吸管理, 嚥下機能障害の実態と対応につき述べる。



## 症状<sup>1)</sup>

初発症状は, 軽度の体重増加不良, 定頸や寝返り, 座位保持の遅れ, 3カ月検診で股関節脱臼等が多い。自発運動が少く, 多くは, 精神遅滞も乳児期から気づかれる。まれに6カ月頃に垂直懸垂で自力で下肢を突っ張り体重支持可能例もあるが, 深部腱反射は乳児期前半を除き消失, ときに原始反射が長期に残存する。

### (1) 筋症状

①顔面筋罹患がある。乳児期には頬部は丸く緊満感があり, 睫毛が内反する。後に鼻唇溝が浅く, 開口し下口唇は外反し厚く流涎が目立つ。学童期前半から頬部は萎縮し, 咬合不全, 開咬, 巨舌, 顎関節の脱臼/亜脱臼も出現。②乳幼児期には徐々に運動機能を獲得し, 3~8歳は本人の最高運動機能を示し(表1a), 学童期以降獲得と逆の順で失う(表1b)。運動機能改善は, 筋変性の進行状態と中枢神経系の発達速度との兼ね合いによる。歩行機能獲得例では定頸獲得が正常である<sup>7)</sup>。③関節拘縮: 乳児期から, 手関節を背屈位にすると指を完全に伸展させることができず, 浅指屈筋, 深指屈筋の短縮が推測される。3歳までには股関節, 膝関節の伸展制限が出現。5, 6歳頃には僧帽筋を硬く触れ, 頸椎の前屈制限が目立つ。8~9歳頃より側弯が出現し, 座位保持時間が長いと側弯を悪化させる。④筋萎縮: 上胸部に目立つ全身性筋萎縮があるが, 多くは一時的に仮性肥大を下腿筋, 前腕筋に認め, また, 四つ這い可能や立位保持可能例では大腿等にも認める。



■表1 福山型先天性筋ジストロフィーにおける運動機能レベルの到達と喪失の平均年齢

a) 各運動機能レベルを獲得する平均月齢				
運動機能レベル	典型例 FCMD (CMD I) 例数	到達平均月齢	良好例 FCMD 例数	到達平均月齢
1 <sup>a</sup>	70	6.56 ± 4.38	11	4.00 ± 1.67
2 <sup>a</sup>	67	16.68 ± 13.99	11	8.64 ± 2.57
3	21	34.95 ± 14.98		
4	38	39.87 ± 18.30	1	9.00
5 <sup>a</sup>	12	44.25 ± 12.58	5	16.00 ± 5.15
6 <sup>a</sup>	2	67.00 ± 7.07	8	23.50 ± 6.59
7	0		10	34.40 ± 11.23
8	0		4	48.00 ± 11.43

b) 各運動機能レベルを喪失する平均月齢				
運動機能レベル	典型例 FCMD (CMD I) 例数	喪失平均月齢	良好例 FCMD (III/IV) 例数	喪失平均月齢
1	2	57.00 ± 4.24	0	
2	9	127.00 ± 25.31	2	150.00 ± 15.56
3	4	90.00 ± 25.35	1	156.00
4	9	100.67 ± 24.69	4	151.75 ± 19.81
5	5	81.20 ± 15.53	4	105.00 ± 24.47
6	1	108.00	7	103.71 ± 18.14
7	0		6	87.67 ± 10.75
8	0		3	78.67 ± 15.95

(Fukuyama et al, 1997)<sup>1)</sup>

## (2) 中枢神経系症状

①知的障害：IQ 30～60。一部を除き社会性、言語理解は比較的良好。情緒は豊かで人なつこい。  
 ②発作：50～60%以上に認める。有熱性痙攣では38℃未満の発熱での誘発例(含：入浴直後の体温上昇時)、24時間以内の反復例、持続時間15分以上例が多く、まれだが痙攣重積による死亡例もある。脳波では、一般に基礎波の速波傾向が目立ち異常紡錘波も認める。しばしば、多焦点性の棘波、棘徐波を認める。初発は2～4歳頃に多く、7歳頃に一時治まるが、投薬を中止すると10代から再び出現する。治療は皮質形成異常に伴うてんかんと同様、抗てんかん薬は生涯必要。筋力低下が著明な場合、発作症状としては「四肢や体幹の緊張や動き」が出現せず、顔面蒼白、眼球固定、流涎等のみとなる。

## (3) 眼科所見

眼振、近視、眼輪筋の筋力低下、睫毛内反、視神経萎縮、黄斑変性、眼底周囲の“丸い病巣”等の報告があり、病理学的には網膜異形成、網膜剝離が確認されている<sup>8-11)</sup>。近視化例が多く、加齢にともない、眼科的異常所見が出現してくる傾向があり、定期的経過観察が重要。

## (4) 心機能

10歳代より心筋障害、10歳代後半より浮腫、頻脈、不整脈、心拡大、心不全症状の報告がある<sup>12)</sup>。車いす生活では、排泄の不便さから、水分摂取が控えられることがあり、下肢静脈血栓、肺梗塞、また尿路結石にも留意する。

## (5) 嚥下障害

嚥下障害のため唾液が気管に流れ込み無気肺を起こしやすい。座位が不安定な時期には、側臥位で、口角から唾液を外へ流出したほうが食べさせ



やすい。進行に伴い嚥下障害を呈し、10代には鼻腔栄養が必要となる。

### (6) その他

中枢神経系以外の奇形性病変には食道裂孔ヘルニア、合指症、口蓋裂、先天性奇形、鎖肛の報告がある。また種々の変質徴候を認める。



## 検査所見

### (1) 血液

血清CK値、アルドラーゼ、AST(GOT)、ALT(GPT)、LDHが新生児期から中等度上昇～高値を示し、幼児期後半以降加齢とともに徐々に低下する。CKアイソザイムではCK-MMが大部分を占め、CK-MBも認める。出産直後では、CKは5万に及ぶこともある。

### (2) 筋CT

下腿最大周径部、大腿中央部、第3腰椎体部、肩甲帯部の検討では、筋CT上低吸収域(LD)と筋断面積の減少(筋萎縮)を認めた。運動機能レベル上昇期でもLDは増強する。典型例ではLD変化は腓腹筋で他のどの部位よりも先行し、ついで大腿、肩甲帯、第3腰椎体の順で認める。同じFKTN異常でも肢帯型では、この傾向は明確でない。

### (3) 筋病理組織所見

新生児から乳児期初期の炎症類似の所見以外、炎症性変化や神経原性変化はなく、筋線維間隙への結合織、脂肪の増多を伴う基本構築の破壊と残存筋線維の減少を認め、年齢とともに高度となる。

### (4) 中枢神経系の病理と頭部画像診断所見

脳重量の減少、短頭を認める。病変の分布および程度は症例により異なるが、中枢神経系の主病変は大脳および小脳のMPG(多小脳回、/厚脳回、II型滑脳症)である。病理では、脳幹で錐体路の走行異常、形成不全、また脳室から少し離れた部位に白質髄鞘の淡明化を認める。MRI上、厚脳回様の部位は皮質が厚く白質の入り込み方が少ない。CT上は造影されないX線低吸収域が、乳幼児の白質部に高率に認められる。左右対称性で、側脳室の後角よりも前角周囲に強く、加齢に伴い

減少傾向を認める。これは新生児期には認めない。水頭症とは無関係で、髄鞘化異常と考えられている。小脳で小嚢胞を多数認める。

### (5) 循環器検査

循環器検査は、胸部X線、心電図、心エコー検査、脳性ナトリウム利尿ペプチド(BNP)採血が主である。BNPは、本症では上昇しにくく、心不全検出の鋭敏度は低いが、上昇時は、高度の心機能低下の存在を示す。



## 日常管理上重要な所見とその治療管理

### (1) ウイルス感染罹患時の急性横紋筋融解症<sup>13,14)</sup>とその治療管理

感染罹患時、主に解熱期に一過性筋力低下を呈する例がある<sup>1,13)</sup>。筋力低下に伴う呼吸不全の可能性に気づき治療管理されなければ死に至る場合もある。発症季節は3～4月、7～8月に多く、発症年齢の平均は3歳6カ月。解熱後に筋力低下の増強が顕在化した例が約半数で、発熱初日から筋力低下に気づくまでの平均日数は3.6日であった。発症前の運動能力の平均はいざり這い以上が多く、創始者染色体をホモ接合に認めた。同エピソードの複数回経験例も多い。治療別回復までに要した期間はステロイド投与群で、非投与群でより早く回復した。発症危険因子として幼児期の夏期の咽頭炎、特にコクサッキーによるヘルパンギーナ等があげられる。筆者ら経験例の遺伝子型はすべてFKTN 3 kb挿入変異をホモ接合体に認めていた<sup>14)</sup>。ステロイド治療群で早期に運動能力回復が認められており、ステロイドによる膜の安定化もしくは筋再生促進が関与している可能性が示唆された<sup>14)</sup>。FKTNの遺伝子異常による肢帯型2例の報告がなされたが<sup>15)</sup>、いずれも同様に発熱を契機に筋力低下を呈し入院を余儀なくされている。ウイルス感染を契機に発症する横紋筋融解症の危険因子として年齢と罹患時期があげられる。発熱時には解熱後も慎重な観察が必要である<sup>15)</sup>。

### (2) 胃食道逆流(GER)とその治療管理<sup>16)</sup>

GERは嘔吐、腹痛、体重減少に加え、貧血や

■表2 慢性呼吸不全の症状

1	息苦しさ
2	朝方の頭痛
3	日中の眠気
4	睡眠障害
5	食欲低下
6	体重減少
7	学習障害
8	疲れやすさ
9	むくみ
10	動悸
11	嚥下障害, 誤飲

誤嚥性肺炎の原因ともなり、QOLを損なう。当科では対象の25%に認め、診断年齢は6カ月～15歳であり、診断年齢は1歳以下と5歳以上に二分された。診断のきっかけは、誤嚥が最多で、次いで嘔気、嚥下困難もあった。クエン酸モサブリドとH<sub>2</sub>ブロッカー内服により治療する。内服治療では効果が不十分な例には腹腔鏡下噴門形成術と、腹腔鏡補助下内視鏡的胃瘻形成術手術治療を行う。当科での手術治療例では、手術後には誤嚥による入院はない。経管栄養はGERの診断後、経口摂取も併用しながら全例で導入し、十二指腸チューブによる導入例もある。

### (3) 呼吸機能障害と呼吸管理

加齢に伴い徐々に呼吸状態が悪化してくる。呼吸管理を考慮すべき症状を表2に示す。重要なものは、朝方の頭痛と日中の眠気、食欲低下、体重減少等である。検査では肺機能検査と血液ガス分析、夜間睡眠中の酸素飽和度と呼気中の二酸化炭素濃度のモニタリングが重要である。呼吸管理導入の目安として、①肺活量が30～50%未満、②二酸化炭素濃度が45～50 mmHg以上、③夜間の酸素飽和度が88%以下で継続する、等がある。肺活量測定が困難な場合も多く、定期的入院で夜間呼吸状態を精査する。

呼吸管理の方法としては、非侵襲的陽圧人工換気(NIPPV)による導入が一般的である。当科におけるNIPPVによる在宅呼吸管理例の検討では、導入年齢はFCMDで8～14歳であった。導入効果としては、食欲増加、体重増加、睡眠障害改善、頭痛改善等が多く、日中のQOLが向上した。合

併症は、マスクの圧迫による皮膚障害、腹部膨満、気胸等である。

夜間睡眠中のみでの使用であっても、導入は、日中覚醒時から行う。マスクに慣れてもらい、不安を取り除くためである。この時期に時間をかけ、最適なマスクを選択し、漏れを最小限にする。順調に慣れたら、呼吸器の条件を順次あげていく(導入圧はIPAP:4～8 cmH<sub>2</sub>O, EPAP:4 cmH<sub>2</sub>O程度)。呼吸器のモードは、補助モード(自発呼吸に合わせて器械が作動)で開始するのが一般的であるが、自発呼吸が弱い場合は、器械が自動的に作動する調節モードのほうがよい場合もある。

NIPPVの導入が困難な場合として、不安が強く、協力が得られない、嚥下障害による誤嚥性肺炎反復、自力排痰困難、慢性呼吸不全が進行し、陽圧を十分にかけても管理できない、等があげられる。NIPPVに固執せず、気管切開術を含めた侵襲的な呼吸管理への移行時期を逸しないことも重要である。生命にかかわりうるので、全身状態に注意し、長期的な視野に立って、医療スタッフが治療方針を共有することが重要である。

### (4) 心機能障害<sup>12,17,18)</sup>

10歳以降は心筋異常が現れることが多い。心機能異常を認めないときは、循環器外来受診の頻度は、10歳以下は1年に1回、10歳以降は6カ月に1回とする。運動機能低下のため運動負荷がなく、心不全の自覚症状は少ない。夜間の寝返り要求回数増加、体重減少傾向、掌の発汗、頻脈、「ため息」は心不全徴候として重要である。アンジオテンシン転換酵素(ACE)阻害薬や、βブロッカーは、短・中期的に心機能を軽度改善しうるが、長期成績や生命予後への効果はいまだ不明である。心機能低下を認めたら循環器小児科医による診察も必要で、心不全の急性増悪での入院時には併診を要請する。心不全の有無にかかわらず、1～3カ月ごとに定期的に外来で、一般状態、栄養、筋力、呼吸状態をチェックし、年に1回、1週間程度、小児科入院し、全身管理、呼吸管理、心機能(血圧、心音異常、肝腫大、末梢冷感に留意、心音減弱、3音の有無、頻拍の有無)をチェックする。

心エコーでは、左室拡張末期径(LVIDd)、短縮



率(LVFS), 壁厚, Myocardial performance index (Tei index) (0.4-0.5 以上では要注意), 左室流入血流(E波, A波), 組織ドプラー(E/e')を測定. 心エコーでLVFSが0.28~0.25以下なら循環器の専門医と相談し, ACE阻害薬, アンジオテンシン受容体阻害薬(ARB),  $\beta$ -ブロッカー, 利尿剤等を用いる. ACE阻害薬エナラプリルでは, 0.15 mg/kgで開始し, 1~2カ月後に0.3 mg/kgまで増量し維持する. 副作用で空咳がときに認められるが, その際は, 循環器専門医に相談し, アンジオテンシン受容体阻害薬(ARB)に変更する. 痩せた児では, より少量から開始. 採血で腎機能や電解質(K濃度)をみながら少量の利尿剤スピロノラクトン(10~25 mg/day前後)を投与(頻尿に注意)する. LVFSが0.25以上に維持できない場合, 心機能がさらに低下すれば, 循環器専門家

に依頼し,  $\beta$ -ブロッカー(Carvedilol)を追加する.



## 予後

厚生省研究班の剖検登録によれば, 死亡年齢は2~27歳に分布し, 平均寿命は14.29  $\pm$  6.18歳. 主な死因は肺炎を含む呼吸不全に次いで心不全が多く, 3%程度の例では10歳前後で死に至る. 当科での最年長齢は38歳である.



## 遺伝相談

多型を用いた連鎖解析により出生前診断が可能な家系がある. 倫理的コンセンサスの問題, 絨毛膜採取による流産誘発の危険性, 判定技術の問題, その後の心理的ケア等課題を残している.

## 文献

- 1) Fukuyama Y et al : Congenital Muscular Dystrophies, Elsevier, 1997, p440.
- 2) Matsumoto H et al : Congenital muscular dystrophy with glycosylation defects of  $\alpha$ -dystroglycan in Japan. *Neuromusc Disord* 15 : 342-348, 2005.
- 3) Yanagisawa A et al : New POMT2 mutations causing congenital muscular dystrophy. *Neurology* 26 : 1254-1260, 2007.
- 4) Silan F et al : A new mutation of the fukutin gene in a non-Japanese patient. *Ann Neurol* 53(3) : 392-396, 2003.
- 5) Murakami T et al : Fukutin Gene Mutations Cause Dilated Cardiomyopathy with Minimal Muscle Weakness. *Ann Neurol* 60(5) : 597-602, 2006.
- 6) 戸田達史 : 福山型先天性筋ジストロフィー. *Clin Neurosci* 17 : 1138-1142, 1999.
- 7) Osawa M et al : Fukuyama type congenital progressive muscular dystrophy. *Acta Paediatr Jpn* 33 : 261-269, 1991.
- 8) Tsutsumi A et al : Ocular findings in Fukuyama type congenital muscular dystrophy. *Brain Dev* 11 : 413-419, 1989.
- 9) 伊藤景子・他 : 福山型先天性筋ジストロフィー症にみられた網膜硝子体異常. *眼科臨床医報* 84 : 526-529, 1990.
- 10) Hino N et al : Clinicopathological study on eyes from cases of Fukuyama type congenital muscular dystrophy. *Brain Dev* 23 : 97-107, 2001.
- 11) 大澤真木子・他 : 福山型先天性筋ジストロフィーの小児・若年者における眼所見. 平成17年度厚生労働省精神・神経疾患研究委託費による研究報告集(2年度班・初年度班, 主任研究者: 川井 充), 2006, p361.
- 12) Nakanishi T et al : Cardiac involvement in Fukuyama-type congenital muscular dystrophy. *Pediatrics* 117(6) : e1187-1192, 2006.
- 13) 池中晴美・他 : 先天性筋ジストロフィーにおける感染症罹患時の一過性筋力低下. *東女医大誌* 70(臨増) : 40-46, 2000.
- 14) Murakami T et al : Rhabdomyolysis induced by Viral Infection in Fukuyama type congenital muscular dystrophy. *Brain Dev*(投稿中)
- 15) Godfrey C et al : Fukutin gene mutations in steroid-responsive limb girdle muscular dystrophy. *Ann Neurol* 60(5) : 603-610, 2006.
- 16) 大澤真木子・他 : 福山型筋ジストロフィー(FCMD)に合併する胃食道逆流(GER)について. 平成17年度厚生労働省精神・神経疾患研究委託費による研究報告集(2年度班・初年度班, 主任研究者: 川井 充), 2006, p360.
- 17) Kajimoto H et al : Beta-blocker therapy for cardiac dysfunction in patients with muscular dystrophy. *Circ J* 70(8) : 991-994, 2006.
- 18) 中西敏雄・他 : 心不全患者の外来管理法. 筋ジストロフィーの心不全治療マニュアルーエビデンスと戦略一, 厚生労働省精神・神経疾患研究委託費「筋ジストロフィー治療のエビデンス構築に関する研究班(主任研究者: 川井 充)」, 2008, pp55-59.

Case report

## A 2-bp deletion in exon 74 of the dystrophin gene does not clearly induce muscle weakness

Shigemi Kimura <sup>a,\*</sup>, Kaori Ito <sup>b</sup>, Hiroe Ueno <sup>a</sup>, Makoto Ikezawa <sup>a</sup>, Yasuhiro Takeshima <sup>c</sup>,  
Kowashi Yoshioka <sup>a</sup>, Shiro Ozasa <sup>a</sup>, Kyoko Nakamura <sup>a</sup>, Keiko Nomura <sup>a</sup>,  
Makoto Matsukura <sup>b</sup>, Koichi Mitsui <sup>a</sup>, Masafumi Matsuo <sup>c</sup>, Teruhisa Miike <sup>a</sup>

<sup>a</sup> Department of Child Development, Kumamoto University Graduate School, 1-1-1 Honjou, Kumamoto 860-0811, Japan

<sup>b</sup> Laboratory of Clinical Pharmacology and Therapeutics, Faculty of Pharmaceutical Sciences, Sojo University, Kumamoto, Japan

<sup>c</sup> Department of Pediatrics, Kobe University Graduate School of Medicine, Kobe, Japan

Received 7 November 2007; received in revised form 10 March 2008; accepted 12 March 2008

### Abstract

Duchenne muscular dystrophy (DMD) is caused by mutation of the dystrophin gene. Cases of dystrophinopathy with a 2-bp deletion in the dystrophin gene commonly result in DMD. We report here a case of dystrophinopathy in a 9-years-old boy with a 2-bp deletion in exon 74 of the dystrophin gene; however, the boy had no clear clinical signs of muscle weakness. Immunohistochemical studies with N-terminal (DYS3) and rod-domain anti-dystrophin (DYS1) antibodies revealed that the dystrophin signals were weaker than in the control sample (non-dystrophinopathy) at the sarcolemma of myofibers, and the studies with C-terminus anti-dystrophin antibody (DYS2) were negative. Our patient's mutation is located between the binding sites of  $\alpha$ -syntrophin and  $\alpha$ -dystrobrevin. These results suggest that this mutation does not clearly induce muscle weakness at least through the age of 9 years. © 2008 Elsevier B.V. All rights reserved.

**Keywords:** Dystrophin; Exon 74; Duchenne muscular dystrophy; Out of frame; Non-muscle weakness

### 1. Introduction

Duchenne muscular dystrophy (DMD) and Becker muscular dystrophy (BMD) are caused by defective expression of the dystrophin gene, resulting in the absence of the dystrophin protein in muscle fibers [1]. DMD results from an out-of-frame deletion(s) in the dystrophin gene resulting in the lack of dystrophin expression in myofibers [2]. The muscle weakness caused by the disease is progressive. The symptoms initially appear as muscle weakness at 2–3 years of age; patients typically lose the ability to walk by themselves before the age of 12. In contrast, BMD, which results from

an in-frame deletion(s) in the dystrophin gene, causes a milder muscle weakness [3]. In skeletal muscle specimens from DMD and BMD patients, necrosis and regenerating fibers are often observed. An immunohistochemical study of DMD with anti-dystrophin antibodies revealed no staining of the surface membrane of the muscle fibers, but a corresponding study of BMD showed weak and patchy staining [4].

Dystrophin binds both to cytoskeletal actin and to the cytoplasmic tail of the transmembrane dystrophin-glycoprotein complex [5], important members of which are  $\alpha$ -,  $\beta$ -dystroglycan,  $\alpha$ -,  $\beta$ -,  $\gamma$ -,  $\delta$ -sarcoglycan, laminin  $\alpha$ 2, and integrin  $\alpha$ 7. In addition, dystrophin also binds to syntrophin and dystrobrevin as a peripheral cytoplasmic subcomplex at exons 73–74 and 74–75, respectively [6,7], which is thought to function like a signaling protein. The members of this subcomplex include neuronal

\* Corresponding author. Tel.: +81 96 3735197; fax: +81 96 3735200.  
E-mail address: kimusige@kumamoto-u.ac.jp (S. Kimura).

nitric oxide synthase (nNOS) and aquaporin-4. Therefore, exon 74 of the dystrophin gene is the key exon. We report here the case of a 9-years-old boy with a 2-bp deletion in exon 74 of the dystrophin gene who shows no clear clinical signs of muscle weakness.

## 2. Methods and case report

### 2.1. Case report

The patient is a 9-years-old boy with no familial history of muscle disease. The patient began to walk independently when he was one-year old. He reported muscle pain in his foot and showed drop foot when he was 2-years old. His family doctor suspected cerebral palsy and referred the boy to our hospital staff to confirm the diagnosis when the patient was 8-years-old. The boy had slight pseudohypertrophy of his calf muscles and mild contracture of his ankle joints, but he did not show Gowers' sign. A manual muscle test did not show muscle weakness. Although the patient could not run fast during the tests, he did exhibit the ability to hop. His Achilles and patellar tendon reflexes were hyperactive, and he had an increased level of serum creatine kinase (1596 U/mL; normal range, 57–284). The results from magnetic resonance imagery of the brain, a chest X-ray, and electrocardiography were normal. The work that the boy has done in school combined with a conversion ability in line with that of normal 9-years-old boys suggests that he does not have mental retardation.

### 2.2. Histological studies and Western blotting analysis for dystrophin

Muscle biopsy specimens were obtained from the biceps brachii according to a standard protocol. The biopsy specimens were studied with hematoxylin and eosin (HE). In addition, immunohistochemical stainings were performed on cryostat sections with monoclonal anti-dystrophin, anti- $\beta$ -dystroglycan, and anti- $\alpha$ -,  $\beta$ -,  $\gamma$ -sarcoglycan antibodies (DYS1, DYS2, DYS3, dystroglycan and sarcoglycan: Novocastra Laboratories Ltd., UK). Western blotting was performed with the antibody against the rod domain of dystrophin (DYS1, Novocastra Laboratories Ltd.).

### 2.3. Mutation analysis of muscle dystrophin gene

Mutational analysis of the dystrophin gene was performed according to the protocol of Surono et al. [8]. The genomic region encompassing exon 74 was amplified by PCR with g74f (5'-CAAATACACTCCTGAGTCCCTAACC-3') as the forward primer and g74r (5'-AGATTCCTGGCACTTTTCTATGTGT-3') as the reverse primer. The amplified product was purified and subjected to sequencing either directly or

after subcloning into a pT7 blue T vector (Novagen, Madison, WI).

## 3. Results

### 3.1. Histological studies

The HE staining of the muscle biopsy (Fig. 1A and B) from the biceps brachii showed slight variations in myofiber size, as well as scattered regenerating fibers and necrotic fibers (Fig. 1B). An immunohistochemical study with anti-N-terminus (DYS3) and anti-rod-domain dystrophin (DYS1) antibodies showed that the immunoreactivity of the patient was weaker (i.e., less staining) than that of the control at the surface membrane of the muscle fibers; but, patchy staining was not observed. Immunoreactivity with antibody for the C-terminus (DYS2) was not observed (Fig. 1C–H). Immunohistochemical studies with anti- $\beta$ -dystroglycan (DG) and anti- $\alpha$ -,  $\beta$ -,  $\gamma$ -sarcoglycan (SG) revealed weaker staining signals for the patient than the control at the sarcolemma of myofibers in skeletal muscle (anti- $\beta$ -,  $\gamma$ -sarcoglycan: data not shown) (Fig. 1I–L).

The Western blotting analysis with DYS1 for dystrophin of skeletal muscle showed that the band size of dystrophin in the patient was almost the same as that of the control and that the quantity of expression in the patient was lower than that of the control (Fig. 2). Again, immunoreactivity with DYS2 was not detected (data not shown).

### 3.2. Mutation analysis of the dystrophin gene

The dystrophin gene of the index case was analyzed for mutations. PCR amplification of all 79 exons did not reveal any deletion mutations. Next, all exons of the dystrophin gene were examined by direct sequencing of PCR-amplified products. In the amplified region encompassing exon 74, two nucleotides (AG) 104 bp downstream or 55 bp upstream from the 5' and 3' ends of exon 74, respectively, were absent (c. 10498–10499delAG), resulting in a frame-shift mutation. This pattern of mutation usually leads to DMD. The mutation is located before the epitope of C-terminus (DYS2), which recognizes amino acids 3669–3685 (nucleic acids 11,004–11,054) in exons 78–79 of dystrophin. These data coincide with immunohistochemical studies.

## 4. Discussion

We report here a case of dystrophinopathy with a 2-bp deletion in exon 74 of the dystrophin gene. The patient's diagnosis should be DMD, as the mutation typically leads to a frame shift in the dystrophin gene. However, the patient does not show any clear clinical signs of muscle weakness at 9 years of age. Western blot-

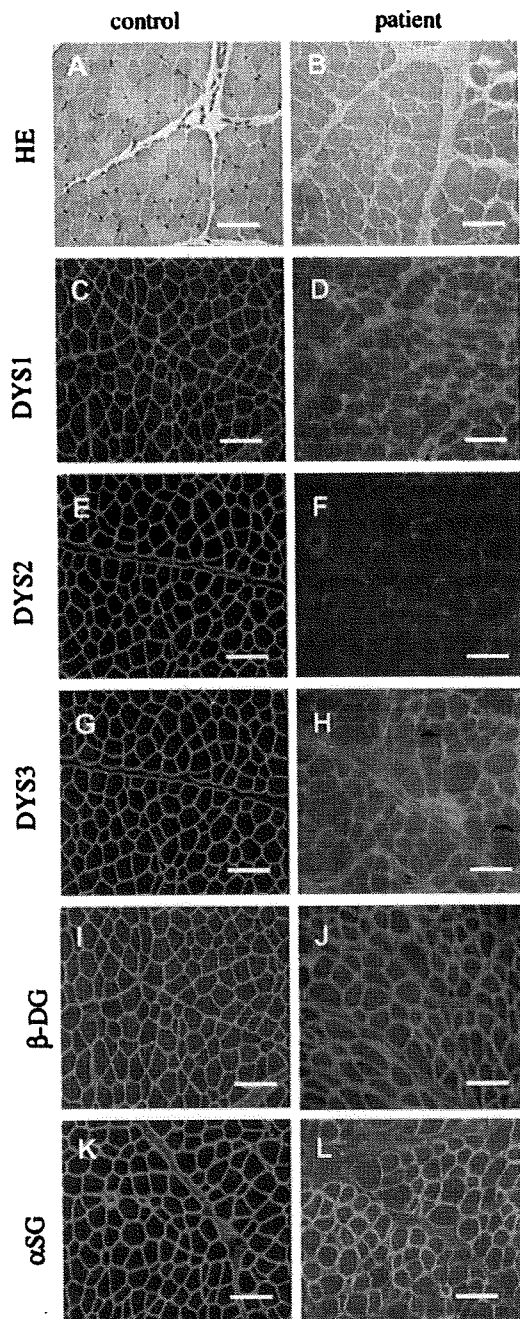


Fig. 1. HE staining and immunohistochemical study. Cryostat sections were prepared from non-dystrophinopathy controls (A, C, E, G, I, K) and patients (B, D, F, H, J, L). HE staining from the patient (B) showed slight variations in myofiber size, as well as scattered regenerating fibers and necrotic fibers. An immunohistochemical study with anti-N-terminus (DYS3), anti-rod-domain dystrophin (DYS1), anti- $\beta$ -dystroglycan ( $\beta$ -DG), and  $\alpha$ -sarcoglycan ( $\alpha$ -SG) antibodies (D, H, J, L) showed that the immunoreactivity of the patient was weaker than that of the control (C, G, I, K) at the surface membrane of the muscle fibers. However, immunoreactivity with antibody for the C-terminus, DYS2 (F), was not detected in the patient. Bar scale, 100  $\mu$ m.

ting analysis of the boy's skeletal muscle tissue demonstrated some expression of dystrophin, albeit low. This

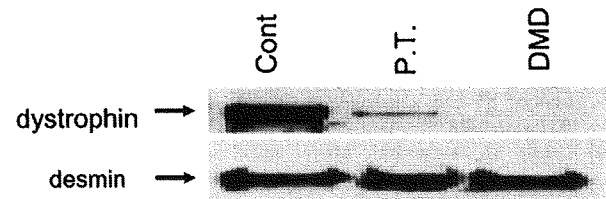


Fig. 2. Western blotting analysis for dystrophin of skeletal muscle. The size of dystrophin from the non-dystrophinopathy control (Cont) and the patient (P.T.) was almost the same; but, the quantity of the dystrophin expression in the patient was lower than that of the control. DMD, Duchenne muscular dystrophy; desmin, internal control.

data suggests that the phenotype more closely resembles BMD than DMD.

The immunohistochemical study of the patient showed that a low level of the dystrophin–sarcoglycan complex at the sarcolemma still remained, because weaker immunoreactivity of  $\beta$ -dystroglycan and  $\alpha$ -,  $\beta$ -,  $\gamma$ -sarcoglycan was observed. Our patient's mutation (c. 10498–10499delAG in exon 74) is located between the binding sites of  $\alpha$ -syntrophin [amino acids 3444–3494 (nucleic acids 10,330–10,482) in exons 73–74] and  $\alpha$ -dystrobrevin [amino acids 3501–3541 (nucleic acids 10,501–10,623) in exons 74–75 of the dystrophin gene] [6,7]. Transgenic mice that express dystrophins with deletions of exons 71–78 (amino acids 3402–3675) had normal muscle function and normal localization of syntrophin and dystrobrevin [9]. These results support the report by Crawford et al. that the dystrophin–sarcoglycan complex may directly bind dystrobrevin, which binds to syntrophin [9]. Our Western blot data also showed that nNOS, which binds to  $\alpha$ -syntrophin, was expressed in the patient's muscle (data not shown). Suminaga et al. reported that a boy with a point mutation (c. C11081T) that produces an aberrant stop codon in exon 76 of the dystrophin gene also does not show muscle weakness [10]. The mild phenotype of our patient may be due to exon skipping excluding exon 74, which results in an in-frame shift of the dystrophin gene (as in the above case). Further experiments are needed to examine this possibility.

We conclude that a deficiency of the cytoplasmic sub-complex of dystrophin that binds to syntrophin and dystrobrevin does not clearly induce muscle weakness, at least through 9 years of age.

#### Acknowledgments

The authors thank Dr. Ryan Pruchnic (Cook MyoSite, Inc., USA) for his assistance. This study was supported by research Grants for nervous and mental disorders and for brain science from the Ministry of Health, Labour and Welfare; and a Grant from the Ministry of Education, Culture, Sports, Science and Technology of Japan.

## References

- [1] Hoffman EP, Brown Jr RH, Kunkel LM. Dystrophin: the protein product of the Duchenne muscular dystrophy locus. *Cell* 1987;51:919–28.
- [2] Koenig M, Beggs AH, Moyer M, Scherpf S, Heindrich K, Bettecken T, et al. The molecular basis for Duchenne versus Becker muscular dystrophy: correlation of severity with type of deletion. *Am J Hum Genet* 1989;45:498–506.
- [3] Becker PE, Kiener F. New X-chromosomal muscular dystrophy. *Arch Psychiatr Nervenkr* 1955;193:427–48.
- [4] Arahata K, Ishiura S, Ishiguro T, Tsukahara T, Suhara Y, Eguchi C, et al. Immunostaining of skeletal and cardiac muscle surface membrane with antibody against Duchenne muscular dystrophy peptide. *Nature* 1988;333:861–3.
- [5] Tinsley JM, Blake DJ, Zuellig RA, Davies KE. Increasing complexity of the dystrophin-associated protein complex. *Proc Natl Acad Sci USA* 1994;91:8307–13.
- [6] Suzuki A, Yoshida M, Ozawa E. Mammalian alpha 1- and beta 1-syntrophin bind to the alternative splice-prone region of the dystrophin COOH terminus. *J Cell Biol* 1995;128:373–81.
- [7] Sadoulet-Puccio HM, Rajala M, Kunkel LM. Dystrobrevin and dystrophin: an interaction through coiled-coil motifs. *Proc Natl Acad Sci USA* 1997;94:12413–8.
- [8] Surono A, Takeshima Y, Wibawa T, Ikezawa M, Nonaka I, Matsuo M. Circular dystrophin RNAs consisting of exons that were skipped by alternative splicing. *Hum Mol Genet* 1999;8:493–500.
- [9] Crawford GE, Faulkner JA, Crosbie RH, Campbell KP, Froehner SC, Chamberlain JS. Assembly of the Dystrophin-associated protein complex does not require the dystrophin COOH-terminal domain. *J Cell Biol* 2000;150:1399–410.
- [10] Suminaga R, Takeshima Y, Wada H, Yagi M, Matsuo M. C-terminal truncated dystrophin identified in skeletal muscle of an asymptomatic boy with a novel nonsense mutation of the dystrophin gene. *Pediatr Res* 2004;56:739–43.



# Clinical outcomes after long-term treatment with alglucosidase alfa in infants and children with advanced Pompe disease

Marc Nicolino, MD, PhD<sup>1</sup>, Barry Byrne, MD, PhD<sup>2</sup>, J. Edmund Wraith, MD<sup>3</sup>, Nancy Leslie, MD<sup>4</sup>, Hanna Mandel, MD<sup>5</sup>, David R. Freyer, DO<sup>6</sup>, Georgianne L. Arnold, MD<sup>7</sup>, Eniko K. Pivnick, MD<sup>8</sup>, C.J. Ottinger, MD<sup>9</sup>, Peter H. Robinson, MD<sup>10</sup>, John-Charles A. Loo, MD<sup>11</sup>, Martin Smitka, MD<sup>12</sup>, Philip Jardine, MD<sup>13</sup>, Luciano Tatò, MD<sup>14</sup>, Brigitte Chabrol, MD<sup>15</sup>, Shawn McCandless, MD<sup>16</sup>, Shigemi Kimura, MD<sup>17</sup>, L. Mehta, MD<sup>18</sup>, Deeksha Bali, PhD<sup>19</sup>, Alison Skrinar, MA, MPH<sup>20</sup>, Claire Morgan, MD, MPH<sup>20</sup>, Lakshmi Rangachari, PhD<sup>20</sup>, Deya Corzo, MD<sup>21</sup>, and Priya S. Kishnani, MD<sup>19</sup>

**Purpose:** A clinical trial was conducted to evaluate the safety and efficacy of alglucosidase alfa in infants and children with advanced Pompe disease.

**Methods:** Open-label, multicenter study of IV alglucosidase alfa treatment in 21 infants 3–43 months old (median 13 months) with minimal acid  $\alpha$ -glucosidase activity and abnormal left ventricular mass index by echocardiography. Patients received IV alglucosidase alfa every 2 weeks for up to 168 weeks (median 120 weeks). Survival results were compared with an untreated reference cohort. **Results:** At study end, 71% (15/21) of patients were alive and 44% (7/16) of invasive-ventilator free patients remained so. Compared with the untreated reference cohort, alglucosidase alfa reduced the risk of death by 79% ( $P < 0.001$ ) and the risk of invasive ventilation by 58% ( $P = 0.02$ ). Left ventricular mass index improved or remained normal in all patients evaluated beyond 12 weeks; 62% (13/21) achieved new motor milestones. Five patients were walking independently at the end of the study and 86% (18/21) gained functional independence skills. Overall, 52% (11/21) of patients experienced infusion-associated reactions; 95% (19/20) developed IgG antibodies to recombinant human lysosomal acid  $\alpha$ -glucosidase; no patients withdrew from the study because of safety concerns. **Conclusions:** In this population of infants with advanced disease, biweekly infusions with alglucosidase alfa prolonged survival and invasive ventilation-free survival. Treatment also improved indices of cardiomyopathy, motor skills, and functional independence. *Genet Med* 2009;11(3):210–219.

**Key Words:** Pompe disease, glycogen storage disease type II, acid maltase deficiency, Myozyme, alglucosidase alfa, lysosomal acid  $\alpha$ -glucosidase, recombinant human GAA, enzyme replacement therapy, cardiomyopathy, motor development

**P**ompe disease is an autosomal-recessive disorder resulting from a lysosomal acid  $\alpha$ -glucosidase (GAA) deficiency. The disease causes lysosomal glycogen to accumulate in various

tissues, particularly muscle, resulting in progressive muscle dysfunction.<sup>1</sup> The rate of disease progression is, in general, inversely related to the amount of GAA activity in fibroblasts. Activity below detection limits leads to rapid accumulation of glycogen in the muscle, resulting in a rapidly progressive disease and early death, whereas patients with detectable low GAA activity tend to experience a slower but relentlessly progressing disease. Regardless of the level of GAA activity, Pompe disease is associated with high morbidity and mortality.<sup>2</sup>

For decades, treatment for all forms of Pompe disease consisted of supportive care to alleviate symptoms. In 2006, alglucosidase alfa, an enzyme replacement therapy (ERT) that specifically targets the underlying cause of symptoms was approved for commercial use in North America and the EU. Alglucosidase alfa provides patients with an exogenous form of GAA in the form of recombinant human (rh) GAA produced in transfected Chinese hamster ovary cells. In a clinical trial of 18 nonventilator-dependent infants treated with alglucosidase alfa beginning at or before 6 months of age,<sup>3</sup> Cox regression analysis showed that treatment with alglucosidase alfa reduced the risk of death by 99% and reduced the risk of death or invasive ventilation by 92% at 18 months of age (both  $P < 0.0001$ ) relative to outcomes in an untreated historic reference cohort. In addition, left ventricular mass was reduced and a subgroup of patients achieved significant gross motor milestones.<sup>3</sup>

Although results from that study were significant, the study population was limited to young infants at the most severe end of the disease spectrum who were at a relatively early stage of disease progression when alglucosidase alfa treatment was initiated. We sought to evaluate whether treatment was safe and effective in patients with Pompe disease when alglucosidase

From the <sup>1</sup>Division of Pediatric Endocrinology, Diabetology and Metabolism, Hôpital Debrousse, University Lyon, Lyon, France; <sup>2</sup>Shands Hospital, University of Florida, Gainesville, Florida; <sup>3</sup>Royal Manchester Children's Hospital, Manchester, United Kingdom; <sup>4</sup>Cincinnati Children's Hospital Medical Center, Cincinnati, Ohio; <sup>5</sup>Rambam Medical Center, Haifa, Israel; <sup>6</sup>DeVos Children's Hospital, Grand Rapids, Michigan; <sup>7</sup>University of Rochester Medical Center, Rochester, New York; <sup>8</sup>University of Tennessee Health Science Center, Memphis, Tennessee; <sup>9</sup>Fort Wayne Neurological Center, Fort Wayne, Indiana; <sup>10</sup>Royal Hospital for Sick Children, Edinburgh, United Kingdom; <sup>11</sup>Long Beach Memorial Medical Center, Long Beach, California; <sup>12</sup>Technical University, Dresden, Germany; <sup>13</sup>Bristol Royal Hospital for Children, Bristol, United Kingdom; <sup>14</sup>University of Verona, Verona, Italy; <sup>15</sup>Hôpital Timone Enfants, Marseille, France; <sup>16</sup>University Hospitals of Cleveland, Cleveland, Ohio; <sup>17</sup>Kumamoto University Graduate School, Kumamoto, Japan; <sup>18</sup>Mount Sinai Medical Center, New York, New York; <sup>19</sup>Duke University Medical Center, Durham, North Carolina; <sup>20</sup>Genzyme Corporation, Cambridge, MA; and <sup>21</sup>Millennium Pharmaceuticals Inc., Cambridge, MA.

Priya S. Kishnani, MD, Department of Pediatrics, Division of Medical Genetics, Duke University Medical Center, Durham, NC 27710. E-mail: kishn001@mc.duke.edu.

Disclosure: P.S. Kishnani, M. Nicolino, and B. Byrne are members of the Pompe Disease Advisory Board for Genzyme Corporation. D. Bali and P. Kishnani have served as consultants for Genzyme Corporation. The clinical trials of Myozyme were supported by grants from Genzyme Corporation at the various sites at which patients were treated. Duke University and inventors of the method of treatment and predecessors of the cell lines used to generate the enzyme used in this clinical trial will benefit financially pursuant to Duke University's Policy on Inventions, Patents, and Technology Transfer, even if those cell lines are not used in the commercialized therapy.

Submitted for publication January 4, 2008.

Accepted for publication October 13, 2008.

DOI: 10.1097/GIM.0b013e31819d0996

alfa therapy was initiated after 6 months of age. The present study was an open-label, multicenter, multinational evaluation of the safety and efficacy of alglucosidase alfa in a heterogeneous population of Pompe patients with onset of symptoms in infancy and evidence of cardiomyopathy who were at variable stages of disease progression (ranging from very advanced and near terminal to less advanced but still with significant effects in a variety of organ systems) when treatment was initiated.

## MATERIALS AND METHODS

### Study design and treatment

Key inclusion criteria were documented onset of Pompe disease symptoms by 12 months of age (corrected for gestation if born before 40 weeks); skin fibroblast GAA activity  $\leq 2\%$  of the normal mean; age 6–36 months at enrollment; and abnormal left ventricular mass indices (LVMI, abnormal value is defined as  $\geq 65$  g/m<sup>2</sup> for patients up to 12 months old or  $>79$  g/m<sup>2</sup> for patients older than 12 months).<sup>4</sup> Patients could be dependent on ventilator support or ventilator-free at enrollment. Exclusion criteria included clinical signs or symptoms of cardiac failure with ejection fraction  $<40\%$ , major congenital anomaly, intercurrent organic disease, and prior treatment with ERT.

Patients were treated with IV alglucosidase alfa (Myozyme<sup>®</sup>, provided by Genzyme Corporation) biweekly for a minimum of 52 weeks. Patients' guardians could then choose to continue treatment under the study protocol. All patients initially received a dose of 20 mg/kg every 2 weeks. After at least 26 weeks of treatment, dose augmentation to 40 mg/kg every 2 weeks was allowed if the patient's clinical condition (motor, cardiac, or respiratory) had significantly deteriorated relative to baseline.

Independent Ethics Committees or Institutional Review Boards at sites in the United States, Europe, and Israel approved protocols and consent forms. Parents or guardians gave written informed consent for patients' participation. Independent boards oversaw safety (Data Safety Monitoring Board) and provided consultation on allergic reactions (Allergic Reaction Review Board). The study is registered at [www.clinicaltrials.gov](http://www.clinicaltrials.gov) as NCT00053573.

### Historical control group

Because infantile-onset Pompe disease is a rapidly fatal disorder and clinical trials have shown that treatment with rhGAA can improve survival, cardiac and respiratory function, growth, and motor development,<sup>5–9</sup> ethics forbade using a placebo group in this study. Instead an untreated historic reference cohort was culled from a group of cases with infantile-onset Pompe disease identified through a retrospective chart review by Kishnani et al.<sup>10</sup> The source group included 168 patients from nine countries and 33 different sites; 55% of patients were born in 1995 or later. The only inclusion criteria for this population were documented GAA enzyme deficiency or GAA gene mutation(s) and onset of signs or symptoms by 12 months of age. This group was screened with additional inclusion and exclusion criteria to closely resemble the clinical characteristics of the treated population in the current study.

Because patients with infantile-onset Pompe disease have a higher risk of death during the first 12 months of life than afterward,<sup>10</sup> survival was analyzed separately for those patients who were  $\leq 12$  months of age at first infusion, those patients who were  $>12$  months of age, and all treated patients. Because of limited availability of detailed data regarding other clinical outcomes in the untreated reference cohort, only survival endpoints were compared with the reference cohort. For all other clinical endpoints, changes in the treated group were compared with baseline.

### Efficacy and safety

The primary efficacy endpoint was the proportion of patients surviving over the course of treatment.<sup>11</sup> Efficacy was further evaluated by measuring invasive and noninvasive ventilator dependency, LVMI, shortening fraction (an alternative to the ejection fraction for describing systolic cardiac function), growth, motor development, functional independence, GAA activity, and glycogen content in quadriceps muscle tissue.

The Alberta Infant Motor Scale,<sup>12</sup> the Peabody Developmental Motor Scale, version 2 (PDMS-2),<sup>13</sup> and the Pompe Pediatric Evaluation of Disability Inventory (PEDI), a disease-specific version of the PEDI,<sup>14–16</sup> were used to assess motor development and functional independence at baseline and at regular intervals thereafter. Motor and cognitive assessments were scored by a central physical therapist. Although not an efficacy endpoint, cognitive function was assessed using the Bayley Scales of Infant Development, 2nd Edition (BSID-II).<sup>17</sup>

Left ventricular mass and shortening fraction were measured by echocardiography. Echocardiograms were read by a central cardiologist who was blinded to patient and time point through Week 52.

To assess safety, patients were observed and vital signs recorded during each infusion and for 2 hours afterward. Adverse events, including infusion-associated reactions (IARs), were continuously monitored in all patients.

Anti-rhGAA IgG antibody formation was assessed with an enzyme-linked immunosorbent assay and confirmed with a radioimmunoprecipitation assay as previously described.<sup>9</sup> Enzyme activity and flow cytometry-based assays were performed retrospectively in all seroconverted patients to detect inhibitory antibodies in patient frozen serum. These two assays were used to characterize antibody response by inhibition of rhGAA enzyme activity and interference with uptake into fibroblasts, respectively.

GAA activity in skin fibroblasts (at baseline) and quadriceps muscle (at baseline and Weeks 12 and 52) was assayed using methods previously described.<sup>9</sup> Cross-reactive immunologic material (CRIM) status was determined as described previously.<sup>9</sup> Briefly, cell lysates derived from patients' fibroblasts were subjected to western blot analysis with a pool of monoclonal antibodies that recognize both native and recombinant GAA; results were confirmed independently by a second laboratory that performed western blot on blinded cell lysate samples using polyclonal antibodies generated against human placental GAA.

### Statistical methods

To include all available follow-up data in the analyses, data were analyzed at various time points, including 52 weeks, 104 weeks, last available follow-up (the last time point at which a given outcome was measured), and end of study. Survival over time and ventilation-free survival were analyzed using Kaplan-Meier time-to-event analysis<sup>11</sup>; the binomial proportions of patients alive and ventilation-free at the end of study were also calculated. A Cox proportional-hazards model<sup>18</sup> incorporating age at diagnosis and age at symptom onset, with treatment duration as a time-varying covariate, was used to compare survival and ventilation-free survival in the study patients to survival in the untreated historical reference cohort.

## RESULTS

### Patient population

Twenty-two patients were enrolled but only 21 were treated, as one patient died of anesthesia-related complications during a procedure to obtain a muscle biopsy before beginning algluco-

sidase alfa treatment. Four age-related protocol deviations were agreed to by the sponsor and the treating physician: three patients were older than 36 months of age (36.6, 37.3, and 43.1 months) and one was 3.7 months of age at the time of first infusion. The older patients all showed significant fine and gross motor development delays, were not able to stand or walk independently, and had LVMI Z scores of at least 5.4; the 3.7-month-old patient already required ventilator support, and so was ineligible for other clinical studies of alglucosidase alfa.

The population was 48% male and predominantly white (Table 1). Baseline GAA activity measured in the skin fibroblasts was negligible (<1%) for all patients; two patients were CRIM negative. The median age at first infusion was 13 months (Table 1). All but one infused patient presented with symptoms by 12 months of age (median 3.0 months; range, 0.0–12.6; ages not corrected for gestational age at birth). One patient was included whose first symptoms were recorded at age 12.6 months, or 12.1 month when corrected for gestational age at birth; although this patient did not meet the age at symptom

onset criterion, the deviation was felt to be quite small and unlikely to affect the study outcome. GAA gene mutations were analyzed in all patients who consented ( $n = 18$ ); each patient had a unique combination of mutations (data not shown) and none had the IVS1 (c.-32-13T→G) mutation that is the most common mutation in adult Pompe patients.<sup>19</sup>

Of the 168 patients in the source population for the untreated historic reference cohort, 84 met the inclusion and exclusion criteria and had survival data; these were used as comparators in the survival analyses. Demographics and baseline characteristics were comparable with the study population (data not shown).

## Efficacy results

### Survival and ventilator use

Fifteen of 21 patients (71%) treated with alglucosidase alfa for a median of 120 weeks (range, 0.6–168 weeks) were alive at the end of the study period. The six patients who died ranged

**Table 1** Patient demographics and baseline characteristics

Parameter	Study population $n = 21$	Untreated reference cohort (for survival analysis only) $n = 86$
Gender, $n$ (%)		
Male	10 (48%)	36 (42%)
Female	11 (52%)	50 (58%)
Race, $n$ (%)		
White	15 (71%)	40 (47%)
Black	2 (10%)	12 (14%)
Hispanic	0	1 (1%)
Asian	3 (14%)	28 (33%)
Other/unknown	1 (5%)	5 (6%)
Age at first symptoms, mo <sup>a</sup>		
Mean $\pm$ SD	3.9 $\pm$ 2.8	3.1 $\pm$ 2.75
Median (min, max)	3.0 (0.0, 12.6)	3.0 (0.0, 12.0)
Age at diagnosis, mo		
Mean $\pm$ SD	8.8 $\pm$ 5.4	5.8 $\pm$ 3.81
Median (min, max)	6.8 (1.5, 22.6)	5.7 (-5.1, 22.7)
Age at first infusion, mo <sup>a</sup>		
Mean $\pm$ SD	15.7 $\pm$ 11.0	
Median (min, max)	13.0 (3.7, 43.1)	
Age at death in historical reference cohort, mo <sup>a</sup>		
Median (min, max)		9.8 (5.9, 47.9)
95% CI		8.6–10.8
Ventilator support at baseline (first infusion)		
Invasive ventilation	5 (24%)	
Noninvasive ventilation	2 (10%)	
No ventilator support	14 (67%)	

<sup>a</sup>Ages are not adjusted for gestational age at birth.

in age from 3.7 to 13.0 months at first infusion and from 7.7 to 27.1 months at time of death. Five of these patients died before 18 months of age and early in the course of treatment (before Week 28); the sixth patient survived until Week 101. The patients who survived ranged in age from 7.0 to 43.1 months (mean, 18.8; median, 16.2) at first infusion and from 34.7 to 80.3 months at study end. None of the deaths were assessed by the treating physician to be related to treatment; causes of death were cardiac and/or respiratory failure in all cases.

Before treatment, of the 21 patients 16 were free of invasive ventilation (two of those 16 patients were noninvasively ventilated, via mask) and five required 24-hour invasive ventilation (via tracheostomy). At the end of the study period, seven of these 16 patients remained alive and free of invasive ventilation, four had become invasive ventilation-dependent, and five had died. Among the five patients who were invasively ventilated at baseline, three continued to require invasive ventilation 24 hours a day, one decreased the number of hours of ventilation from 24 hours to 12 hours, and one died (Table 2).

The Kaplan-Meier survival estimate at 104 weeks, the last evaluable time point, was 71.1% (95% [confidence interval] CI: 51.6–90.6%) for study patients, compared with 26.3% (95% CI: 6.5–46.1%) in the reference group (Table 3). When patients were divided by age at first infusion, there was no overlap between the 95% CIs for the 104-week survival estimates between the study group and the reference group. Cox regression analysis<sup>18</sup> comparing treated patients with patients in the historical reference group indicated that treatment with alglucosidase alfa reduced the risk of death by 79% ( $P = 0.0009$ ) and the risk of death or invasive ventilation by 58% ( $P = 0.0207$ ) over the course of the study (Table 4). Note that the risk of death or invasive ventilation in the study group was compared with risk of death only in the historical reference group, because reliable information on ventilation status was not available. Risk reduction for death or any type of ventilation was not statistically significant.

### Cardiac response

At baseline, all patients showed evidence of left ventricular hypertrophy (abnormal LVMI and LVM Z score  $>2$ ) as assessed by the enrolling sites. This assessment was confirmed by a central, blinded cardiologist who concurred with the sites in 18 of 19 cases where echocardiograms were of sufficient quality to allow reassessment; one patient had a baseline LVM Z score of 1.7 on reassessment. Over the course of the study, mean LVMI improved steadily, resulting in a 42% reduction by Week 52 and a 63% reduction by Week 104 (Table 5). Beyond Week 12, all patients with echocardiograms who had elevated LVMI experienced further decreases in LVMI and those who were within the normal range maintained normal LV mass. By the time of last echocardiography assessment, 81% (17/21) of patients showed a reduction in LVM, including 12 patients who achieved normal LVM (Z score  $<2$ ; Fig. 1). Of the four patients in whom LVM did not decrease, one died before any repeat assessment, and the other three died before the Week 24 assessment. Mean shortening fraction (SF) Z score at baseline was  $-1.2$ . After an initial drop, SF also improved over time (Fig. 1, Table 5), with mean SF increasing over baseline by 22% at Week 52 and 30% at Week 104.

Baseline and follow-up LVM Z scores were also analyzed for patients according to age at first infusion. Mean LVM Z score at baseline was  $6.7 \pm 1.64$  for patients  $\leq 12$  months of age at first infusion ( $n = 9$ ) and  $4.2 \pm 2.45$  for patients  $>12$  months of age at first infusion ( $n = 10$ ), suggesting that younger patients had more rapid disease progression. At 52 weeks, only four patients

in the younger group had evaluable echocardiograms; for these patients mean LVM Z score had decreased to  $2.5 \pm 3.5$ . The mean LVM Z score at 52 weeks for patients  $>12$  months of age at first infusion ( $n = 9$ ) was  $1.6 \pm 1.91$ . No evaluation of statistical significance for the change over time between the two groups was attempted because of the small sample size.

### Muscle GAA activity and glycogen content

Mean GAA in muscle at baseline was  $12.5 \pm 11.0$  nmol/hour/g. By Week 52, all patients receiving repeat biopsies ( $n = 13$ ) experienced a marked increase in GAA activity with mean levels of  $89.9 \pm 32.2$  nmol/hour/g. Mean glycogen value in muscle by biochemical analysis at baseline was  $7.1 \pm 2.5\%$ . After 52 weeks of treatment, 13 patients had repeat biopsies assessed: glycogen content decreased for six patients, remained stable for three patients, and increased for four patients relative to baseline, and mean glycogen decreased to  $5.0 \pm 2.4\%$  (Table 2).

### Motor development

Thirteen of 21 patients (62%) had measurable motor development gains (AIMS and/or PDMS-2 gross and fine motor skills) as determined by increases in age-equivalent scores from baseline to end of study. Of the 13 patients with significant motor gains, five patients had functional use of the legs and were walking independently and eight patients had functional use of the neck, trunk, and upper extremities and were sitting at the end of the study (Table 2). The remaining eight patients (38%) made no significant motor development gains from baseline. At baseline, these eight patients had median muscle GAA activity below quantifiable levels; they also had generally lower motor scores at baseline (data not shown). The 13 patients who had measurable motor development gains had higher baseline median muscle GAA activity (15.6 nmol/hour/g tissue versus below quantifiable levels) and better motor scores at baseline (data not shown). Five of these 13 patients were younger than 12 months old at the time of their first infusion, and five of the seven patients who did not have measurable motor gains were also under 12 months of age at first infusion (Table 2).

### Functional independence skills

Pompe PEDI scores steadily increased over the course of the study indicating the acquisition of functional skills. From baseline to last assessment, 17 of 21 patients (81%) demonstrated consistent gains in at least one of the domains assessed, indicating increased ability to independently perform activities of daily living related to mobility, self-care, and/or social function. Three of the four patients without gains died before Week 24 assessment.

Two of 11 patients who were older than 12 months at time of first infusion showed no improvement in Pompe PEDI scores. Of those nine who did improve, six showed measurable improvement in all three domains assessed. Of the 10 patients younger than 12 months at first infusion, three showed improvements in all three Pompe PEDI domains.

### Physical growth

Growth in body weight and length generally progressed over the course of the study (Fig. 2). By last assessment, age-equivalent weight values were at or above the third percentile in 81% (17/21) of patients. Results for age-equivalent length were similar, with 90% (19/21) of patients at or above the third percentile at last assessment. Two patients started below the third percentile in weight, did not improve, and died with  $<16$  weeks on therapy; one patient declined in age-equivalent weight and subsequently died after 28 weeks on therapy. One patient